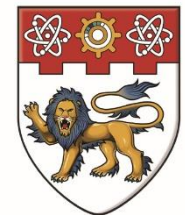

NANYANG TECHNOLOGICAL UNIVERSITY

DESIGN OF FRONT-END RECEIVER FOR LOW NOISE ULTRASOUND IMAGING SYSTEM

SUN HUAXI

SCHOOL OF ELECTRICAL AND ELECTRONIC ENGINEERING

A thesis submitted to the Nanyang Technological University
in fulfilment of the requirement for the degree of
Master of Engineering

2016

Acknowledgments

I would like to express my sincere gratitude to the people and organizations that support me during my study.

First of all, I would like to thank Prof. Zheng Yuanjin for his great guidance as my supervisor.

Secondly, I want to thank MediaTek Singapore Pte Ltd and EDB for the scholarship.

Besides, I'm grateful for the help from Dr Tangkai, Dr Lou Liheng, Dr Gao Fei, Dr Chen Bo, Dr Wang Yong and Dr Feng Xiaohua. They are my seniors and colleagues who teach me a lot during my work.

Last but not the least, I hope to say thanks to NTU and the staff for providing good environment and support for students.

Table of Contents

List of Figures

List of Tables

Abstract

Ultrasound imaging has been widely used in industrial and biomedical applications. In general, high sensitivity of the front-end system is always wanted. The way of increasing the sensitivity is to increase the input signal and reduce the noise figure (NF) of the system that is dominated by NF of the first stage. Therefore the ultrasound transducer, the low noise amplifier (LNA) and the matching network between them are studied, resulting in the conclusion that conventional matching techniques are insufficient for voltage amplification or noise optimization.

This thesis presents a novel way of input matching to increase sensitivity. Capacitors and inductors with negligible noise are used to pre-amplify the ultrasound signal and reduce NF by making the input-referred noise of LNA less significant. The front-end design includes transducer modeling, LNA design and co-design of input matching network. Ultrasound transducer model is successfully extracted by experiment with 95% accuracy. A LNA with $0.9\text{nV}/\sqrt{\text{Hz}}$ input-referred noise is designed and simulated in standard 0.18μm process. The input matching technique is verified by simulations and experiments, showing that it can provide over 15dB voltage gain and 6dB signal-to-noise ratio (SNR) improvement. Related materials have been patented.

Chapter 1 Introduction

1.1 Motivations and Objectives

The front-end of ultrasound imaging system basically includes an ultrasound transducer, a low noise amplifier and the matching network. An ultrasound transducer is a device which can convert electrical signal into ultrasonic waves and vice versa. It is used as a transmitter to emit and receive the ultrasound signal for imaging. The reflected signal is sometimes as small as several μV which is not easy to detect and susceptible to noise.

Ultrasound imaging system is widely used in various industries such as flaw detection, weld inspection, tissue examination and so on. The ultrasound transducer is basically a mechanical device whose characteristics are determined by parameters of the materials. Since the transducer serves as the receiver of the front-end, its electrical model is always of interest. The imaging system captures the voltage or current signal and forms an image based on the quality of the electrical signal. Therefore, a conversion from the mechanical model of the ultrasound transducer to an electrical model is required to be performed at the beginning, followed by proper design of the circuits for first-stage amplification.

There are some problems that need to be resolved. First of all, an efficient and accurate way of modeling the ultrasound transducer is demanded. However, the manufacturers of ultrasound transducer and circuit designers have different concerns which creates the gap during the mechanical to electrical conversion. The manufactures provide specifications such as center frequency, waveform and spectrum while the circuit designers care more about the impedance

characteristics and noise performance. One way of generating the electrical model of the ultrasound transducer is to conduct synthesis and derive the electrical parameters in terms of physical parameters of the material. This method is not widely adopted for a few reasons. The most obvious reason is that the synthesis is not always performed by the device manufacturers because the electrical properties are not of their concerns. Besides, the physical properties of the materials may vary after being integrated into a package which at the same time introduces parasitic effects. Thus, the accurate electrical model of the ultrasound device could only be extracted by measuring the electrical characteristics after fabrication.

The theory of the electrical model of ultrasound transducer is founded but there are few documents explaining how to get exact values of those model parameters such as impedance, inductance and capacitance through the measured impedance characteristics. The more important thing is that the reported modeling methods are not general enough to cover all multi-resonance conditions of the piezoelectric materials. Most revealed methods only introduce the steps to model ultrasound transducer with single resonance, which will be explained further in Chapter 2. Sometimes there is a parasitic shunt resistor in addition to the basic model but sometimes there is not, which could be solely determined after measuring the ultrasound transducer. Thus, there is a need to summarize and derive a simple, systematic and accurate modeling method applicable to general transducers.

The second problem is that the matching technique currently adopted in ultrasound front-end receiver is not optimized. Common matching techniques such as impedance matching and 50Ω power matching are inherited directly from RF techniques that are not tailored for ultrasound

transducers since the electrical model of the transducer is unique and quite different from antenna's model. Few studies of ultrasound matching in the literature imply that there is plenty of space to make improvement by optimizing the overall front-end design of ultrasound imaging system.

The author is inspired to co-design the matching network with LNA and transducer to achieve a low noise system with high sensitivity. Conventional matching technique in RF design aims to get maximum power transfer but the input voltage is halved. A novel technique named "resonance matching" is applied with ultrasound transducer to reduce NF and amplify input voltage. The task comprises transducer modeling, matching network design and LNA design.

1.2 Major Contribution of the Thesis

For circuit designers to integrate the front-end system, the electrical model of the transducer must be known as the premises because the matching shall be crafted to cater the model in order to get the best results. The theory of transducer model is established though, but the lack of generosity and simplicity is still to be addressed. All transducers studied in the thesis are purchased from market which is the common practice for designers to implement a customized system. The author would like to claim to be the first one to provide simple and detailed procedures to extract all parameter values of the electrical model of transducer with double resonances. The validity of the claim is supported by the fact that in the literature, no such procedures are reported for the transducer with double resonances. Even for extracting a

transducer with single resonance, the procedures are tedious.

The focus of this thesis is on inventing a new matching technique for ultrasound transducer. The basic electrical model of ultrasound transducer is different from antenna's model which is simply a 50Ω resistor. Therefore, directly applying RF matching techniques here is not the best choice. The working frequency of ultrasound transducer is much lower than that of RF device. Normally, the frequency range of ultrasound is from 0.5MHz to 20MHz, and the input impedance of LNA need not to be 50Ω. Besides, the structure of ultrasound pre-amplifier is also different from RF LNA. Since there are so many differences, the author invents a novel matching technique based on the transducer's electrical model and co-design considerations with the LNA.

The LNA implemented in this thesis serves as an auxiliary part to elaborate the co-design with the matching network and it is not taped out. The LNA shall always be implemented in the front-end system and the point is that by using the novel matching technique, the NF will be reduced. Thus, the LNA adopts the structure which is beneficial for resonance matching and it is tuned to achieve low NF.

This thesis aims to prove that the new matching technique proposed by the author can provide voltage gain as well as NF reduction. To fulfill this purpose, the new matching technique is compared to existing matching techniques. Results obtained with and without this new matching technique are presented to show its effectiveness. Since this is a new exploration, there is no specifications prescribed as the improvement of adopting the new matching technique depends on specific conditions of the ultrasound transducer and LNA used in the

system. The thesis offers the general analysis and demonstration of the new matching technique. Major contributions are listed below.

Firstly, the author develops an effective way for ultrasound transducer modeling with over 95% accuracy. Before this, there is no systematical method revealed for constructing the electrical model of ultrasound transducer. Now, by measuring the impedance of the ultrasound transducer, the electrical model of the mechanical device could be built accurately.

Secondly, a novel matching technique is invented which can increase the input voltage signal and reduce NF of the ultrasound system significantly. The matching provides over 15dB gain and 6dB SNR improvement in the experiments.

Lastly, a LNA is designed and simulated in 0.18μm CMOS process with input-referred noise of $0.9\text{nV}/\sqrt{\text{Hz}}$. Simulations results have shown that resonance matching can truly reduce NF of the front-end.

1.3 Organization of the Thesis

Literature review is presented Chapter 2 with comments on prior art.

Ultrasound transducer modeling method is explained in Chapter 3.

Chapter 4 is the major part which elaborates the resonance matching technique.

Results are shown in Chapter 5 which demonstrate the validation of the proposed matching

technique.

Chapter 6 is about the LNA design for ultrasound imaging application.

The last part, conclusion, is in Chapter 7.

Chapter 2 Literature Review

2.1 Piezoelectric Micromachined Ultrasonic Transducer (pMUT)

Bulk piezoelectric ceramic materials are mostly applied in traditional ultrasound transducer fabrication. The acoustic coupling is poor and it is expensive to map into 2D transducer arrays. In the contrast, micromachined ultrasonic transducers having the compliant membrane structures, can be designed for good acoustic coupling and fabricated by IC technology [1]. MUTs can be mainly classified into two types according to their mechanisms: capacitive MUT (cMUT) and pMUT [2].

Since the output pressure of cMUT depends quadratically on the excitation voltage and the inverse of the capacitor gap, cMUT designs normally have submicron gaps resulting in complicated fabrication [3]. The linear displacement range related to the gaps is especially significant in air-coupled transducers which limits the output power. To overcome the problem, some air-coupled capacitive transducers apply bias voltages of hundreds of volts, which increases system complexity [4].

Piezoelectric micromachined ultrasound transducers (pMUTs) do not require high bias voltage.

The pMUT's linear displacement range is a function of the membrane thickness [5], and it could be easily increased at the sacrifice of reduction in the electromechanical coupling factor. Thus, pMUT is more popular in most applications and the study is focused on pMUT here.

2.2 Equivalent Circuit Model of pMUT

Normally, major parts of pMUT include a piezoelectric film and electrodes, supported by a silicon membrane. The device structure of a commercial pMUT is shown in Figure 1. Simply speaking, the working principle of pMUT is that the electrical excitation signal applied to the pMUT will cause vibration of the membrane, generating ultrasonic wave to propagate to the target. When receiving, the reflected ultrasonic wave gives pressure to the membrane, inducing charges on the electrodes which will be picked up as an electrical signal for imaging processing. It will be much easier to design the circuit if the mechanical and electrical parameters could be unified and therefore, constructing an electrical model of the mechanical device is necessary.

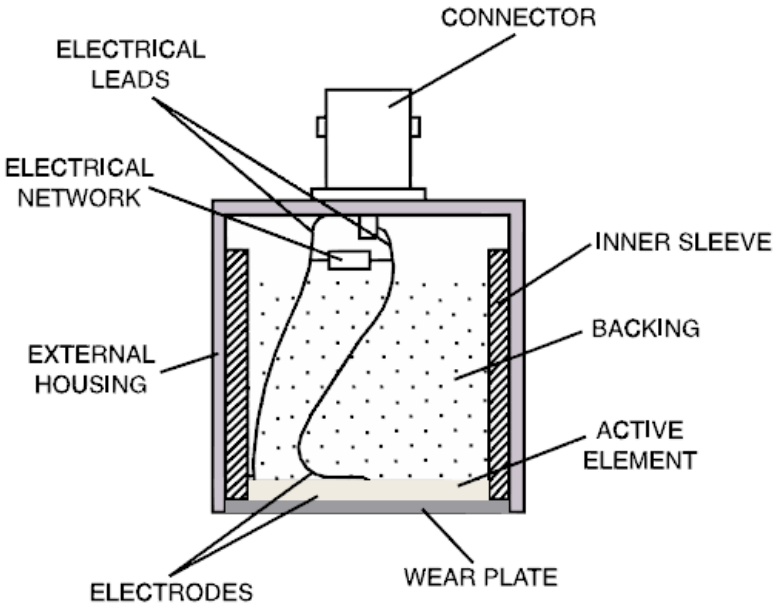

Figure 1. Typical device structure of a commercial pMUT

The reason why the mechanical model could be converted to an electrical model is explained here. pMUT in resonance state could be modeled with one degree of freedom as in Figure 2 [6]. The model includes mass *M* representing the mass of the energy converter, a damper with coefficient of friction *R* and spring with coefficient of mechanical sensitivity *K*.

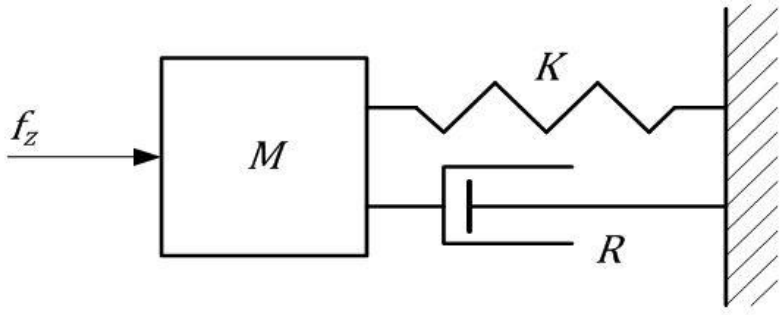

Figure 2. Mechanical model of pMUT

There are four forces existing in this system: the external force f_Z, the force of elasticity f_K, the force of friction f_R and force of inertia f_M, which satisfy the following equation:

$$f_Z = f_M + f_R + f_K \tag{1}$$

Defining:

x – deviation from the equilibrium position

v – linear velocity of particles

F_{ZM} – amplitude

ω– pulse of this force

t – time

Equation (1) could be written as:

$$f_Z = M\frac{d^2x}{dt^2} + R\frac{dx}{dt} + \frac{1}{K}x = M\frac{dv}{dt} + Rv + \frac{1}{K}\int_{-\infty}^{t} v d\tau \tag{2}$$

Assuming the vibration external force is sinusoidal:

$$f_Z = F_{ZM}\sin\omega t \tag{3}$$

By representing those variables in complex form:

$$\underline{F_Z} = j\omega M\underline{V} + R\underline{V} + \frac{1}{j\omega K}\underline{V} \tag{4}$$

Complex mechanical impedance of the transducer is:

$$\underline{Z_{mech}} = \frac{\underline{F_Z}}{\underline{V}} = R + j\omega M + \frac{1}{j\omega K} \tag{5}$$

The above equation is very similar to the form of electrical impedance of a serial RLC circuit in Figure 3.

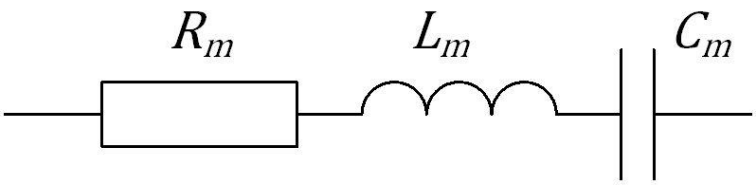

Figure 3. Serial RLC circuit

$$\underline{Z_m} = R_m + j\omega L_m + \frac{1}{j\omega C_m} \tag{6}$$

The linear velocity has the greatest amplitude when the mechanical impedance value Z_{mech} is the smallest. It happens at the condition:

$$f_M + f_K = 0 \tag{7}$$

In piezoelectric activity, the relation between the external force and the intensity of the electric filed induced is linear. A coefficient of proportionality k_p could be defined that:

$$f_Z = uk_p \tag{8}$$

where u is the induced voltage of pMUT.

The electrical charge induced on pMUT is proportional to the deformation, so:

$$q = k_p x \tag{9}$$

According to the definition of current:

$$i = \frac{dq}{dt} = k_p \frac{dx}{dt} = k_p v \rightarrow v = \frac{1}{k_p} i \tag{10}$$

By substituting equation (8) and (10) into equation (2):

$$k_p u = \frac{M}{k_p} \cdot \frac{di}{dt} + \frac{R}{k_p} i + \frac{1}{k_p K} \int_{-\infty}^{t} i(\tau) d\tau \tag{11}$$

$$u = \frac{M}{k_p{}^2} \cdot \frac{di}{dt} + \frac{R}{k_p{}^2} i + \frac{1}{k_p{}^2 K} \int_{-\infty}^{t} i(\tau) d\tau \tag{12}$$

The voltage of serial $R_m L_m C_m$ circuit is:

$$u = L_m \frac{d^2 q}{dt^2} + R_m \frac{dq}{dt} + \frac{q}{C_m} = L_m \frac{di}{dt} + R_m i + \frac{1}{C_m} \int_{-\infty}^{t} i(\tau) d\tau \tag{13}$$

By comparing equation (12) and (13), it could be derived:

$$L_m = \frac{M}{k_p{}^2}, R_m = \frac{R}{k_p{}^2}, C_m = k_p{}^2 K \tag{14}$$

The mechanical impedance of the vibration system has the same form as the electrical impedance of a serial RLC circuit and the values of the electrical parameters could be determined by the corresponding mechanical parameters according to equation (14). Therefore, the mechanical model of pMUT could be converted to an electrical model. Basically, there is another shunt capacitor in the electrical model that represents the static capacitance of the

piezoelectric material clipping by the electrodes.

Single Resonance Model

Butterworth first raised that the mechanically vibrating system with a single resonance, driven by electric filed of a capacitor, could be represented by an equivalent model at its terminals [7]. Later, Van Dyke introduced a circuit with constant value elements which was identical to Butterworth's. The Butterworth-Van Dyke (BVD) model shown in Figure 4 was verified by experiments [8].

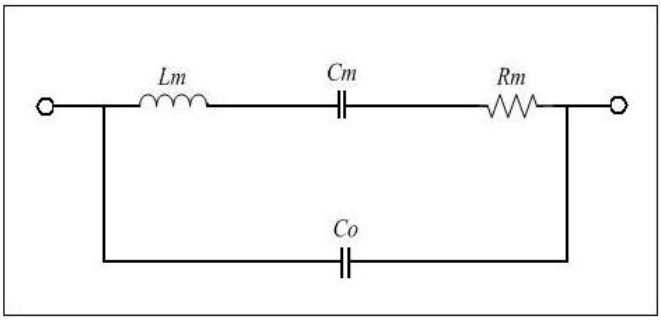

Figure 4. BVD model with a single resonance

C_0 represents the static capacitance of the piezoelectric material while the mechanical vibrating system is modeled by a series RLC. L_m describes the mass of the mechanical system. R_m and C_m vary to model the changes in boundary conditions. R_m is called the emission resistance:

$$R_m = R_{lm} + R_{xm} \tag{15}$$

R_{lm} represents the loss in piezo-material and R_{xm} represents the acoustic transmission into the medium [9]. In this way the coupling between electrical part and mechanical part is represented. The input impedance of ultrasound transducer is:

$$Z = \frac{(\omega^2 C_m L_m - 1) - j(\omega R_m C_m)}{(\omega^2 C_m C_0 R_m) + j[\omega^3 C_m C_0 L_m - \omega(C_m + C_0)]} \tag{16}$$

The transducer has a serial and a parallel resonance frequency:

$$\omega_s = \frac{1}{\sqrt{L_m C_m}} \tag{17}$$

$$\omega_p = \sqrt{\frac{C_m + C_0}{L_m C_m C_0}} \tag{18}$$

$$\frac{\omega_p}{\omega_s} = \frac{f_p}{f_s} = \sqrt{1 + \frac{C_m}{C_0}} \tag{19}$$

At those frequencies, the magnitude of impedance Z displays certain pattern shown in Figure 5. The serial resonance frequency is the optimal operating frequency of such mechanical system because oscillation magnitude is maximized at this point. At this frequency, L_m and C_m will cancel each other from impedance aspect [10].

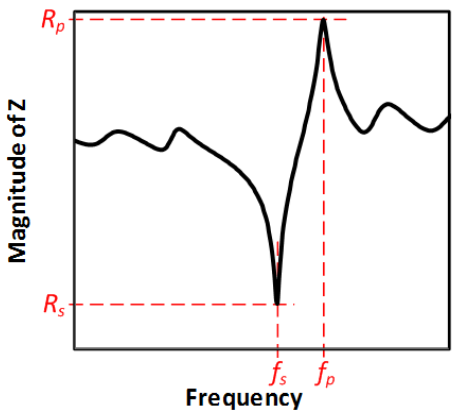

Figure 5. Magnitude of transducer impedance at resonance frequencies

Multiple Resonances Model

Sometimes, the piezo-material exhibits multiple resonances in a single mode. Butterworth was the first person to describe it in Figure 6. The model includes a static capacitor shunted by an infinite number of serial RLC with one series representing each resonance [11]. In fact, it is hard to predict at the beginning whether the transducer has single resonance or multiple resonances because the property of material will be influenced during fabrication. A systematical method of determining the resonance model and its element values is described in Chapter 3.

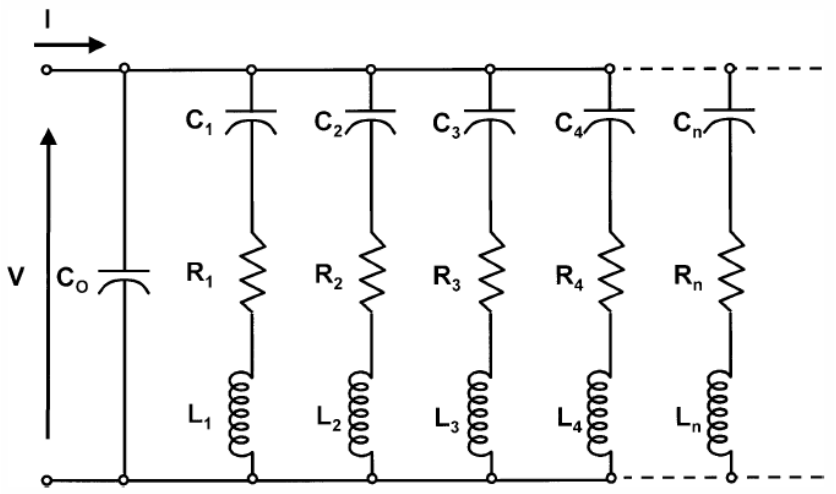

Figure 6. BVD model with multiple resonances

2.3 Exiting Matching Techniques in Ultrasound Systems

Common impedance matching techniques such as “L” matching (Figure 7) or transformer matching (Figure 8) are used with pMUT. In such cases, the input impedance of LNA is designed to be 50Ω and the impedance of pMUT is matched to 50Ω by adding reactive components. Some transducer manufacturers simply use a 50Ω shunt resister which means

X_a=0 and X_b=50Ω in Figure 7. The power match seems to be plausible but the voltage at input terminal of LNA is halved.

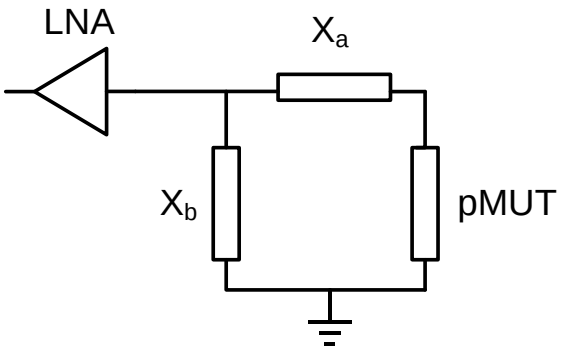

Figure 7. "L" matching technique

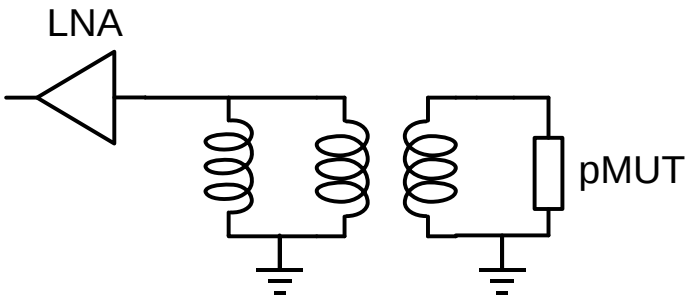

Figure 8. Transformer matching technique

Conventional ultrasound frequency range is below 20MHz indicating that the design need not follow the RF principle. The signal from pMUT is mainly voltage and the input impedance of LNA could be very high. Instead of power match, high input voltage is wanted and the input impedance of LNA is preferred to be high enough.

The well-known noise match theory states that NF is the lowest when source impedance $R_s = \frac{v_n}{i_n}$, where v_n and i_n are input-referred voltage and current noise of LNA respectively.

However, this technique has certain limitations when applied in ultrasound field. For high impedance analog LNA, exact noise match is not practical because the matching inductor may be too large to implement. Another issue is noise matching does not guarantee voltage gain. In contrary, the proposed matching technique in Chapter 4 provides predictable voltage gain and NF reduction at the same time and it could be applied flexibly.

2.4 Passive Amplification Method in Other Fields

Passive amplification was mentioned in few papers, none of which had revealed the essence of the method though. The basic ideal was to use one inductor and one capacitor to achieve voltage amplification without introducing much noise if quality factor *Q* of the inductor was acceptable. When the LC resonated in Figure 9, the voltage at LNA's input was very large, given that the input impedance of LNA was super high rather than 50Ω.

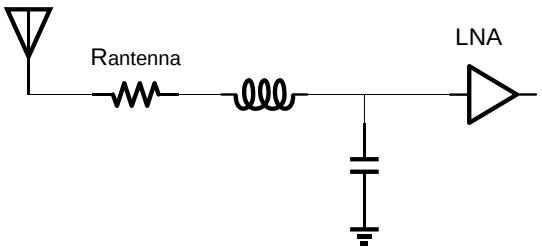

Figure 9. Passive amplification by using LC resonance circuit

In [12], they did not investigate the influence of LNA input impedance or the advantage of passive amplification in noise figure reduction.

In [13], they seemed to use resonance circuit to get voltage amplification but it turned out to

be a fail practice. After simplification, their structure could be represented in Figure 10. They intentionally added a low *Q* inductor with parallel resistance of 630Ω to resonate with parasitic input capacitor of LNA. Some matching network was used to match 630Ω with antenna's impedance (50Ω). They claimed for achieving both highest possible voltage amplification (10dB voltage gain) and preventing signal reflection at the same time. However, it was just the resistor termination approach, abandoned long time ago. There was no power reflection but power waste on R_p. This R_p also introduced extra noise figure of 3dB. The reason why there was certain voltage amplification was that the matching network transformed 50Ω to 630Ω, elevating the output voltage of antenna at the same time. What they conducted was basically not passive amplification because the core of passive amplification method was transforming source impedance (typically 50Ω) to a large value by using a resonance LC circuit with negligible parasitic resistance. It should amplify the voltage a lot without degrading the noise figure.

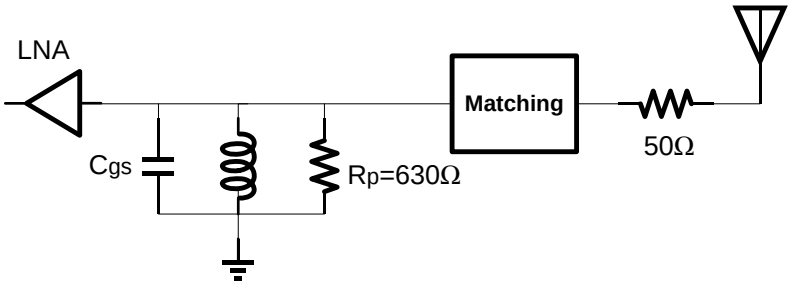

Figure 10. Resistor termination matching

In [14], passive amplification was proposed to reduce noise figure of the system in a similar manner. The flaw was that they thought the input impedance of LNA ought to be infinite to have minimum noise figure but the input impedance had no effect on noise figure actually.

They also omitted the influence of current noise, which was significant under high impedance condition.

In summary, the principle of passive amplification method still remains unclear in the literature. The fundamental theory is not well explained and its advantages have not been fully explored. The proposed resonance matching technique is invented by the inspiration of passive amplification but it is indeed different. The differences will be explained in Chapter 4.9 and this novel method will be compared with existing methods introduced above.

Chapter 3 Ultrasound Transducer Modeling

In the literature, it has been proven that the mechanical model of pMUT could be converted into an electrical model. However, the mechanical parameters may vary during fabrication process, which makes it difficult to get the electrical parameters based on equation (14). Besides, there is a shunt capacitor and sometimes a shunt resistor in addition to the serial RLC circuits whose values could only be determined by measuring the impedance of the pMUT. The number of resonances of pMUT is also unknown before measurement. Though the theory is there, the author develops a systematic method to extract the electrical model by only measuring the impedance of pMUT. The pMUT used here is a typical one available in the market.

The working frequency of pMUT is normally from 0.5MHz to 20MHz, and the fractional bandwidth can exceed 50%. This method could model the pMUT accurately across the full

bandwidth.

3.1 A General Approach for Transducer Modeling

Ultrasound transducer is used as the transmitter in imaging system. It transforms electricity into ultrasound waves through mechanical vibration. Its electrical model needs to be identified for co-design with the LNA. A general approach proposed by the author for transducer modeling is presented in this chapter.

A transducer has one port for electrical signal while the other port is for acoustic signal. If the mechanical part is modeled by electrical components (RLC) as illustrated in literature review, it could be treated as a one-port electrical device. Since it is a passive device, its internal structure is characterized by its impedance. A commercial ultrasound transducer, part number V311 from Olympus shown in Figure 11, is tested for modeling.

Figure 11. Commercial ultrasound transducer

The impedance is measured by network analyzer through a standard RG-58 cable. Calibration is performed to eliminate the influence of the cable. Basic electrical models introduced in Chapter 2.2 are used as references. Some initial values are assumed in the reference model and

the input impedance of the model is simulated in Advanced Design System (ADS). The simulated impedance is then compared with the measured input impedance. Iterations of tuning are performed to match the simulated impedance with the measured one. If finally these two are almost the same, it means the model is correct. Otherwise the model needs to be adjusted.

Single resonance model is assumed at the beginning. Initial values of the components in Figure 1 are calculated from the measured data by following steps. The operating frequency of the transducer is 10MHz from its data sheet. The input impedance (Z) of the transducer is measured by network analyzer when sweeping frequency from DC to 15MHz. In Figure 1, C_m and L_m will resonate with each other at the serial resonance frequency which is also the operating frequency. C_0 is the static capacitance of piezoelectric material, which is much larger than C_m according to device physics. When observing magnitude of Z, the influences of C_m and L_m only appear significantly near parallel resonance frequency f_p and serial resonance frequency f_s. At other frequencies, the pattern of magnitude of Z behaves more like a single capacitor C_0. Thus, at low frequencies near DC, measured Z could be used to calculate the estimated value of C_0. C_m is then estimated by observing the distance between the two resonance frequencies in Figure 5. Equation (19) is used to calculate C_m and equation (17) is used to calculate L_m. Large value of R_m will make the upper and lower peak less obvious, meaning a more plat figure line of Z. A random but reasonable value (100Ω) is assigned to R_m. Now, all values in Figure 1 are obtained.

3.2 Model Simulation and Optimization

The electrical model is built with 95% accuracy. At low frequencies near DC, the author finds that *Z* seems to be purely resistive. If the conventional BVD model is valid, *Z* should be purely capacitive at low frequencies. Therefore, the author suggests there should be a shunt resistor R_s in parallel with C_0 shown in Figure 12.

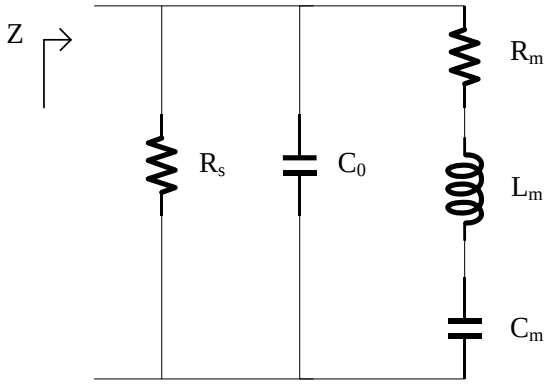

Figure 12. Single resonance ultrasound transducer model with shunt resistor

Initial value of R_s is just the value of *Z* at DC and C_0 could be estimated by using value of *Z* at 1MHz. The impedance of the model in Figure 12 is simulated by substituting all initial values calculated before. Optimum tuning of components' values is executed to get maximum matching. In Figure 13, the simulation results are represented by red line and compared to the measured impedance which is the blue line. Figure 13 (a) plots the magnitude of *Z* while Figure 13 (b) plots the phase of *Z*, both of which need to be matched for a successful modeling.

Simulated impedance Measured impedance

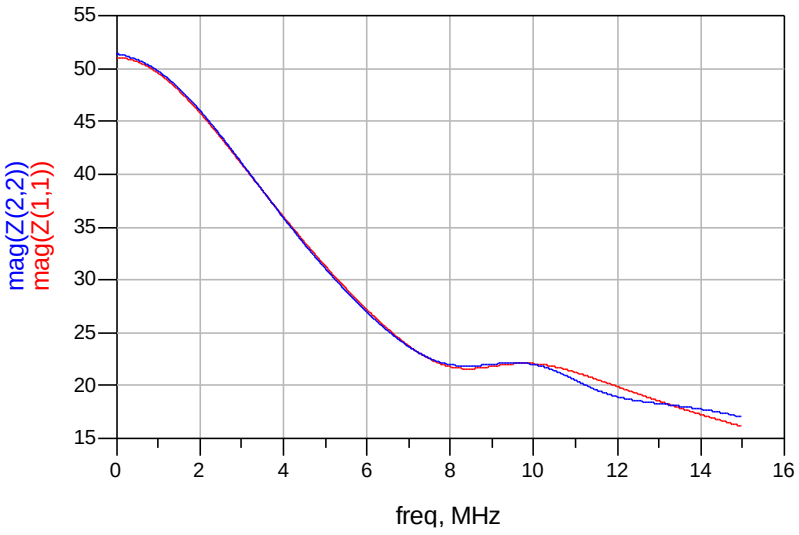

Figure 13 (a). Comparison of $|Z|$ between simulated data and measured data (single resonance)

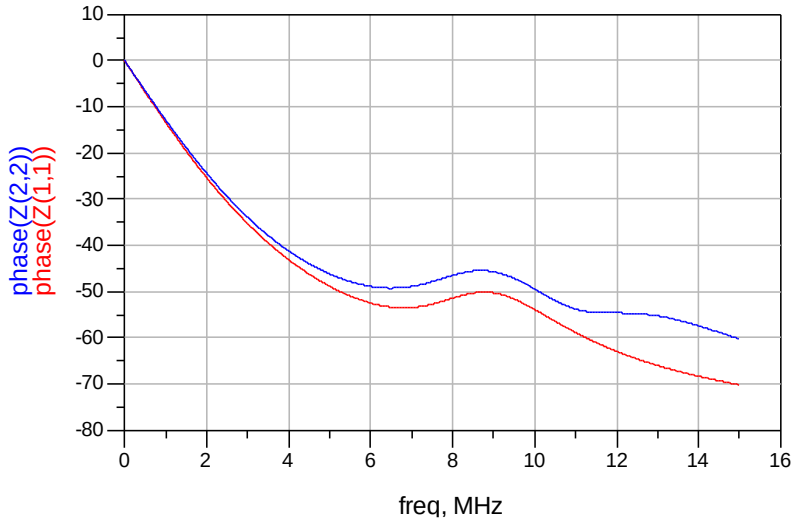

Figure 13 (b). Comparison of $\angle Z$ between simulated data and measured data (single resonance)

It could be seen that the magnitude of *Z* can match very well while the phase of *Z* deviates a lot even after optimum tuning. The reason is that the transducer actually has two resonances instead of one. When analyzing Figure 13 (a) carefully, there is a serial resonance peak at 8.5MHz and a parallel resonance peak at 9.5MHz approximately. They both belong to the first resonance. Later, the second serial resonance appears at 12MHz and the second parallel resonance appears at 14MHz. These two form the second resonance. This could also be identified in Figure 13 (b). One resonance provides one local minimum and one local maximum. Therefore, by observing the input impedance of ultrasound transducer, the number of resonances could be determined. Identical piezoelectric material in different ultrasound transducers may have a random number of resonances and it could only be determined after measuring.

A double resonances model shown in Figure 14 is simulated and tuned. The results are compared with the measured impedance in Figure 15. It can be clearly seen that the simulated data and measured data are almost coincident. In fact, 95% of the simulation data points fit in with the measured data with errors less than 5%. Those are systematic errors which are unavoidable.

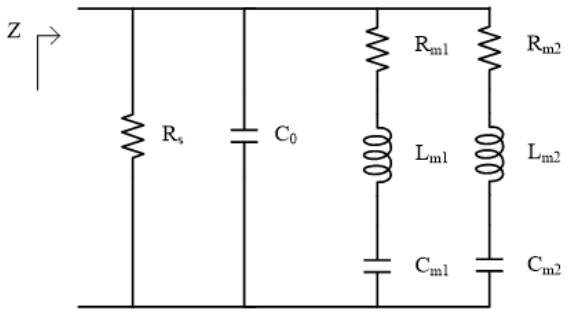

Figure 14. Double resonances ultrasound transducer model with shunt resistor

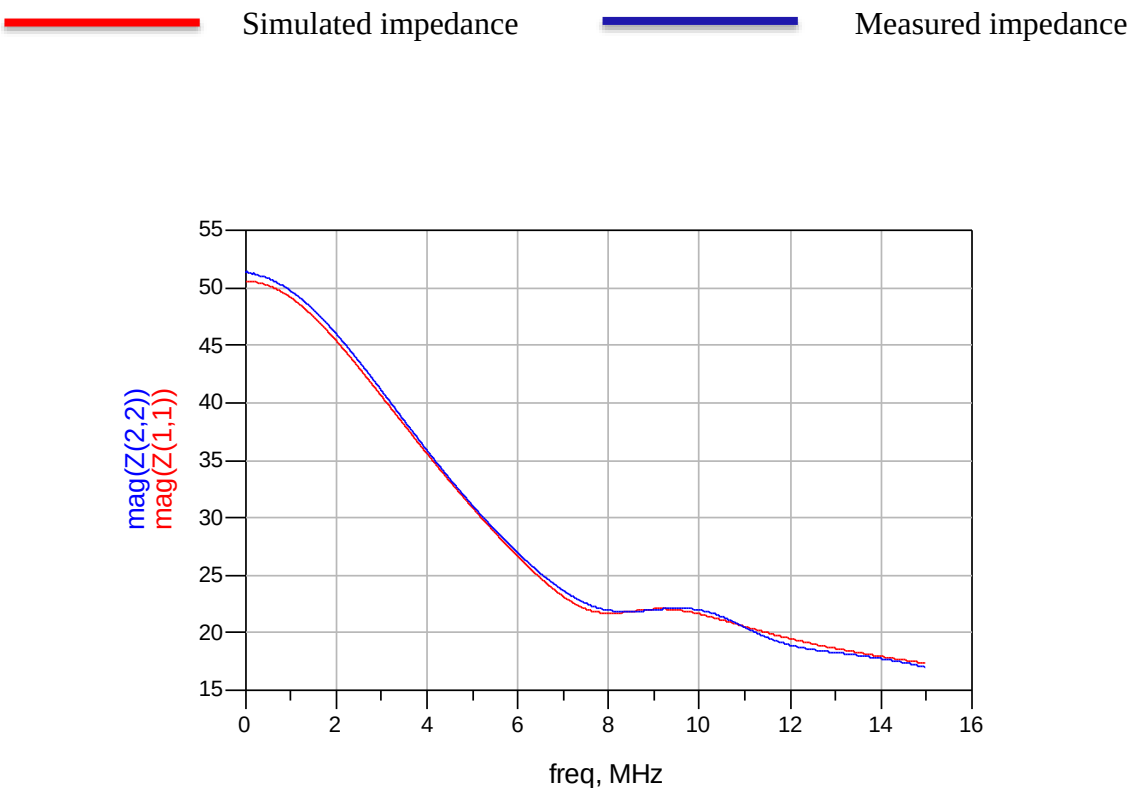

Figure 15 (a). Comparison of |*Z*| between simulated data and measured data (double resonances)

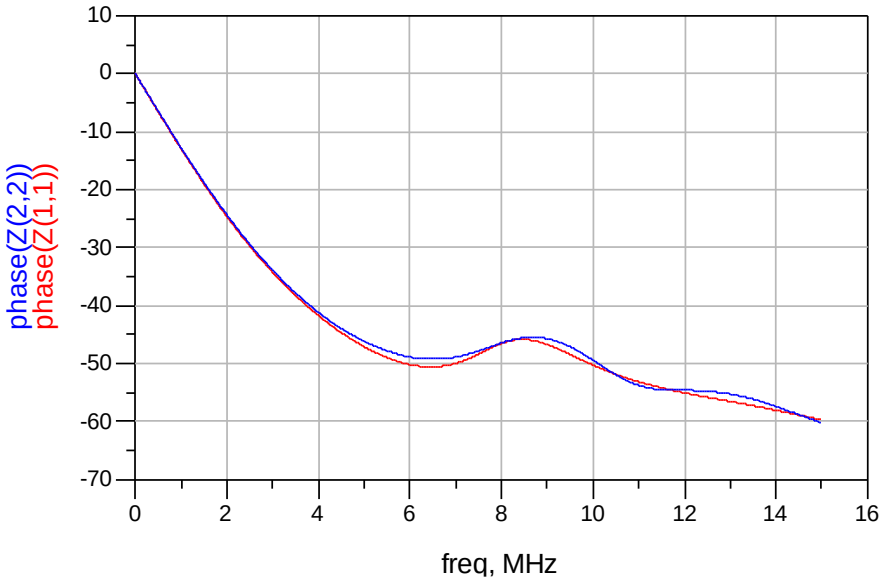

Figure 15 (b). Comparison of $\angle Z$ between simulated data and measured data (double resonances)

It turns out that the model extracted by the author is very accurate and the general approach established for ultrasound transducer modeling is applicable. The number of resonances of the piezoelectric material is determined by counting the number of local minimum (or local maximum) points. The ultrasound transducer tested in this experiment has a double resonances structure. It contains passive components whose values are shown in Table 1. R_s is close to 50Ω so it is believed to be added intentionally for power match.

Component	Value
R_s	50.58Ω
C_0	569.08pF
R_m	115.354Ω
L_m	1.473μH
C_m	87.99pF
R_{m1}	113.824Ω
L_{m1}	5.488μH
C_{m1}	69.90pF

Table 1. Components' values of the ultrasound transducer model

Chapter 4 Resonance Matching Technique

The author proposed a new matching technique named “resonance matching”. The novelty is that by using multi-order LC ladder, the impedance of pMUT is raised to a large value instead of 50Ω. Then the signal will be amplified passively and NF will be reduced. A thorough study of this technique is presented in this chapter with experiment results showing its usefulness.

Under some circumstances like deep penetration, the signal received by the ultrasound transducer is very small which requires the system to have high sensitivity. For pMUT, the electrical signal is the induced voltage across the piezoelectric material, and therefore the maximum voltage is wanted at LNA’s input.

4.1 Voltage Amplification Derivation

To have the maximum voltage at LNA’s input, the input impedance of the LNA should be as high as possible to minimize loading effect. A common source (CS) amplifier is a good choice. The operating frequency of ultrasound transducer is normally below 20MHz, at which the CS amplifier’s input impedance could be treated as infinite. By using inductors and capacitors, the voltage could be raised to a large value at certain frequency. For simplicity, conventional BVD model with single resonance is used for explanation at the beginning. A general condition is discussed later.

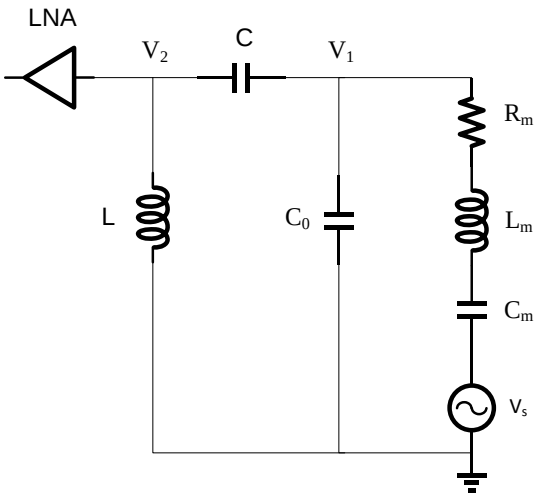

Figure 16. Illustration for voltage amplification

The circuit is shown in Figure 16. At operating frequency ω_s, L_m and C_m will cancel each other. V_s is the received signal source in the ultrasound transducer. LC components are assumed to be ideal and the input impedance of LNA is assumed to be infinite. Equations for voltage amplification are derived. Voltage gain is α. By Kirchhoff's law:

$$\frac{V_1 - V_s}{R_m} + V_1 j\omega_s C_0 = (V_2 - V_1) j\omega_s C \tag{20}$$

$$-(V_2 - V_1) j\omega_s C = \frac{V_2}{j\omega_s L} \tag{21}$$

Inductor value is selected as:

$$\omega_s^{\,2} = \frac{1}{L\dfrac{C_0 C}{C_0 + C}} \tag{22}$$

Solving those equations results in:

$$\alpha = \frac{V_2}{V_s} = \frac{C_0}{C} + 1 \tag{23}$$

Another configuration for voltage amplification is shown in Figure 17.

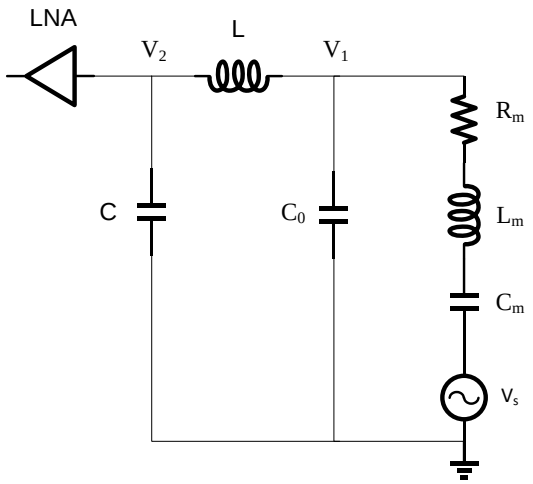

Figure 17. Another configuration for voltage amplification

By applying Kirchhoff's law:

$$\frac{V_1 - V_s}{R_m} + V_1 j\omega_s C_0 = \frac{V_2 - V_1}{j\omega_s L} \tag{24}$$

$$-\frac{V_2 - V_1}{j\omega_s L} = V_2 j\omega_s C \tag{25}$$

Inductor value is selected as:

$$\omega_s{}^2 = \frac{1}{L\dfrac{C_0 C}{C_0 + C}} \tag{26}$$

This time the voltage gain is:

$$\alpha = \frac{V_2}{V_s} = -\frac{C_0}{C} \tag{27}$$

From equation (23) and (27), the voltage gain could be set according to the ratio of C_0 to C. It should be noted that passive network does not provide any power gain, the voltage gain is achieved at the cost of current reduction.

4.2 Non-ideal Inductor Effect

The finite quality factor of inductor will affect the voltage amplification. Actually α is always smaller than the calculated value, taking the actual condition in Figure 18 for illustration:

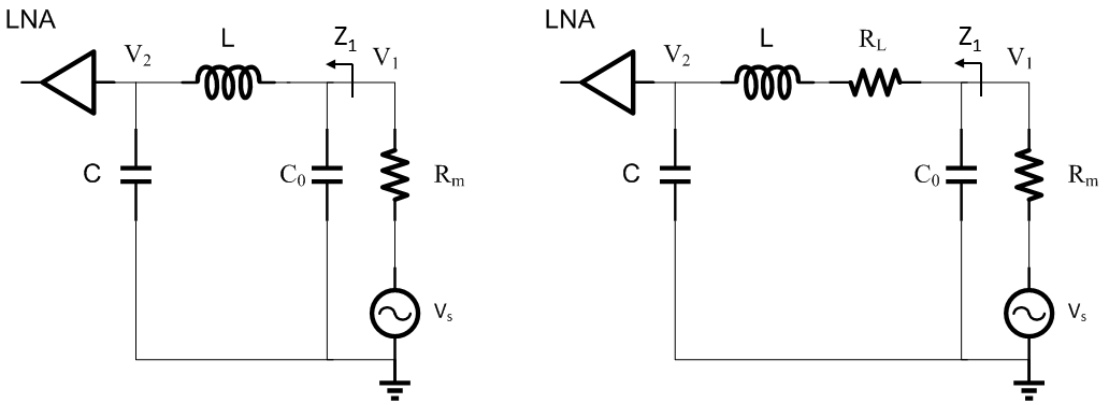

Figure 18. Finite quality factor of inductor degrades α

In Figure 18, if the inductor is ideal and equation (26) is applied, Z_1 will be infinite at ω_s. V_s is equal to V_1 and α is independent of R_m as the equation (27) shows.

$$\alpha = \frac{V_2}{V_1} \times \frac{V_1}{V_s} \tag{28}$$

Finite quality factor of inductor degrades α involving R_m. If the inductor is non-ideal with a parasitic resistor R_L, things are different. Z_1 is not infinite in this case and thus V_s is no longer equal to V_1 ($\frac{V_1}{V_s} < 1$). Z_1 and R_m forms an impedance divider and any increase in R_m will decrease $\frac{V_1}{V_s}$ as well as α. Any increase in R_L will also decrease α because it makes $\frac{V_2}{V_1}$ smaller. Some simulation results shown in following tables support the findings. The transducer discussed here is another one whose center frequency is 5MHz.

ω_s (Hz)	C_0 (pF)	C (pF)	L (μH)	R_L (mΩ)	R_m (Ω)	$\|\alpha\|$ (dB)	Ideal $\|\alpha\|$ (dB)
5M	4000	100	10.3855	1	10	30.1	32
					1000	3.96	

Table 2. R_m degrades voltage gain

ω_s (Hz)	C_0 (pF)	C (pF)	L (μH)	R_m (Ω)	R_L (Ω)	$\|\alpha\|$ (dB)	Ideal $\|\alpha\|$ (dB)
5M	4000	100	10.3855	10	0.001	30.1	32
					1	29.17	
					5	25.7	

Table 3. R_L degrades voltage gain

In Table 2, when R_m increases from 10Ω to 1000Ω, voltage gain decreases from 30.1dB to 3.96dB drastically. In Table 3, voltage gain decreases as R_L increases, in a milder manner. It could be concluded that R_m and R_L should be minimized for voltage amplification.

4.3 Impedance Transformer

The essence of voltage amplification is through impedance transformation. For example, the resistor and capacitors in Figure 16 form an impedance transformer shown in Figure 19.

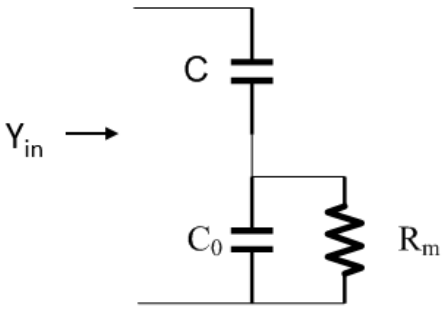

Figure 19. Impedance transformer

Its admittance is:

$$Y_{in} = G_{in} + jB_{in} = \frac{j\omega_s C - \omega_s{}^2 R_m C C_0}{j\omega_s R_m (C + C_0) + 1} \tag{29}$$

$$G_{in} = \frac{\omega_s{}^2 R_m C^2}{\omega_s{}^2 R_m{}^2 (C + C_0)^2 + 1} \tag{30}$$

$$B_{in} = \frac{\omega_s C + \omega_s{}^3 R_m{}^2 C C_0 (C + C_0)}{\omega_S{}^2 R_m{}^2 (C + C_0)^2 + 1} \tag{31}$$

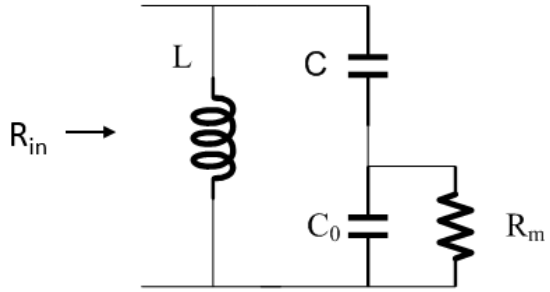

Figure 20. Use a shunt L to cancel the imaginary part

If a shunt inductor is added to cancel the imaginary part as Figure 20, the resistance and inductance are:

$$R_{in} = R_m(1+\frac{C_0}{C})^2 + \frac{1}{\omega_S{}^2 R_m C^2} \tag{32}$$

$$L = \frac{1}{\omega_s B_{in}} \tag{33}$$

What the matching network does is to raise R_m to R_{in}. Since power is constant if LC are ideal, voltage is amplified accordingly. This could be explained by Thévenin's theorem as Figure 21 illustrates:

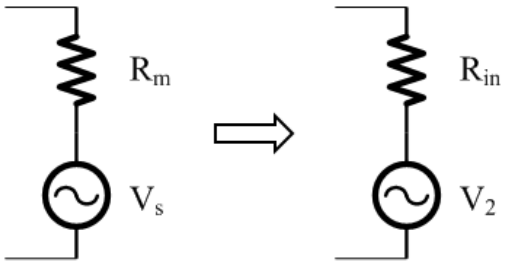

Figure 21. Thévenin's equivalent circuit

$$P = \frac{V_s^2}{R_m} = \frac{V_2^2}{R_{in}} \tag{34}$$

The output impedance is transformed from R_m to R_{in} and open terminal voltage is amplified from V_s to V_2.

It is important to note that the inductor value used here is defined by equation (33) instead of equation (22). Equation (33) defines the optimal inductance because under this condition, the inductance resonates with the equivalent capacitance and the impedance is purely resistive.

Figure 22 is simulated in ADS to view impedance transformation and voltage amplification.

ω_s (Hz)	C_0 (pF)	C (pF)	V_s (V)	R_m (Ω)
5M	4000	100	1	10

Table 4. Parameters in simulation

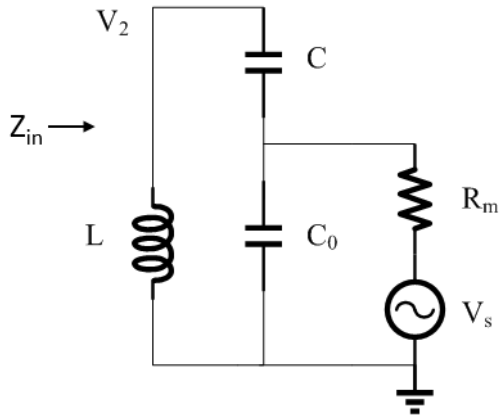

Figure 22. Simulation for impedance transformation and voltage amplification

Results of Z_{in} are plot in Figure 23 and results of V_2 are plot in Figure 24. The results when the inductor value is calculated by equation (22) are plot in red line while that calculated by equation (33) are in blue.

L by equation (22) L by equation (33)

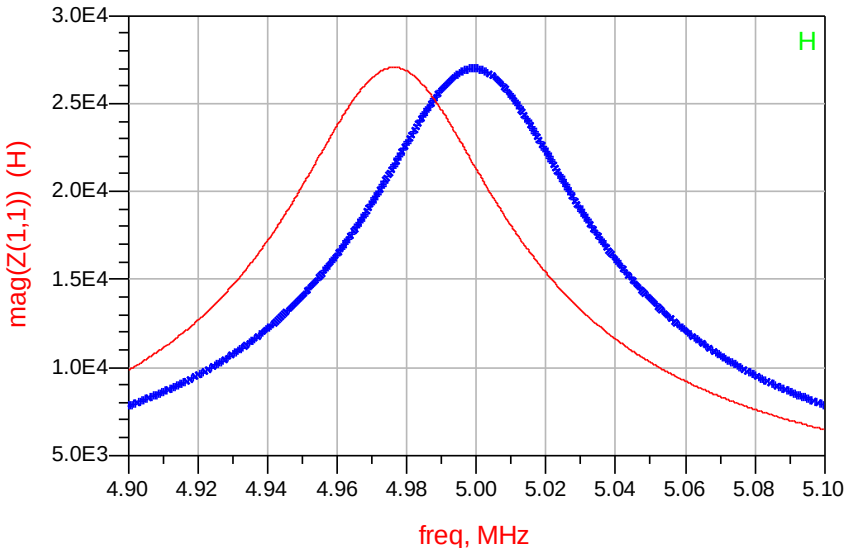

Figure 23 (a). Magnitude of transformed impedance Z_{in}

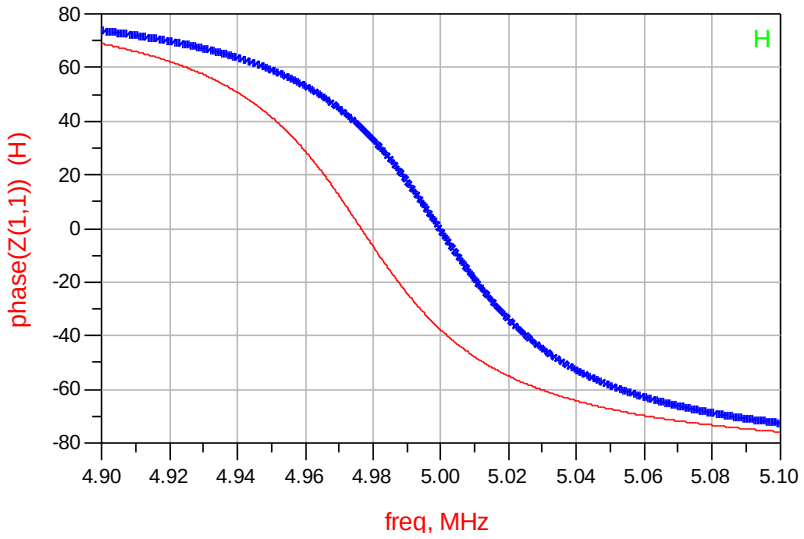

Figure 23 (b). Phase of transformed impedance Z_{in}

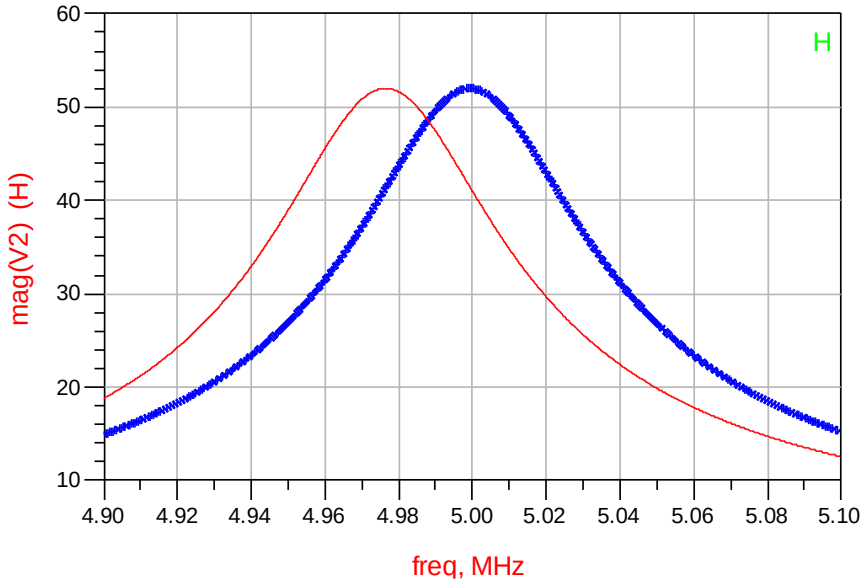

Figure 24 (a). Magnitude of open terminal voltage V_2

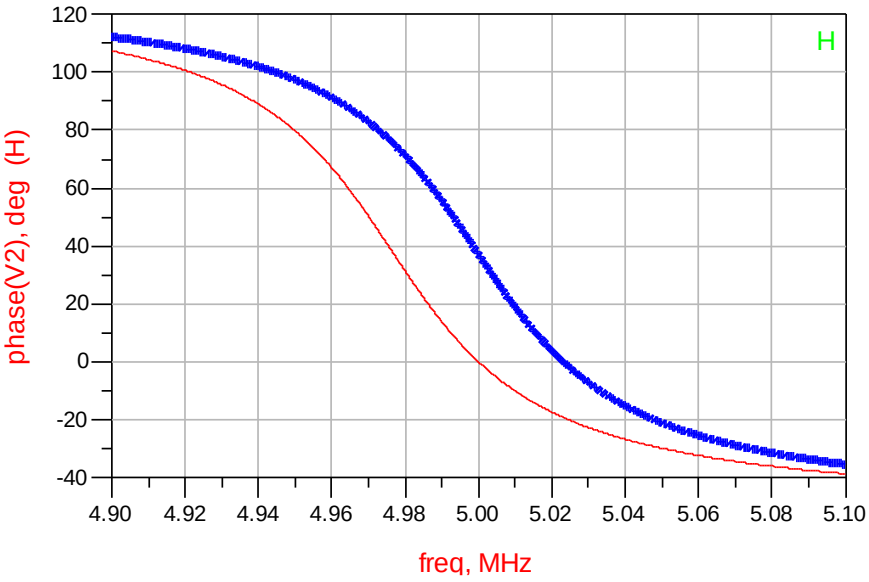

Figure 24 (b). Phase of open terminal voltage V_2

From the red line in Figure 23, it could be seen that L does not resonate with the equivalent capacitance at 5MHz. At 5MHz, Z_{in} is a complex number but α is an integer (α=41). The resonance frequency is 4.976MHz where the peak of $|Z_{in}|$ appears. The red line in Figure 24 shows that $|V_2|$ at 5MHz is also smaller than that at 4.976MHz, which is expected. The resonance frequency is smaller than ω_s because the equivalent parallel capacitance is larger than $\frac{CC_0}{C+C_0}$. At resonance frequency, $R_{in} > R_m(1+\frac{C_0}{C})^2$ thus $|\alpha| > 1+\frac{C_0}{C}$.

When L is calculated by equation (33), it resonates with the equivalent capacitance at 5MHz and Z_{in} is purely resistive. The blue line in Figure 24 indicates the voltage gain is maximum at resonance but α is a complex number now.

Then it is clear that L should resonate with the equivalent capacitance at ω_s to have maximum voltage amplification (maximum $|Z_{in}|$ and maximum $|\alpha|$). The reason why equation (22) is presented at the beginning is that it is an approximation of equation (33) when the quality factor Q_m of ultrasound transducer is high. Q_m is defined by:

$$Q_m = R_m \omega_s C_0 \tag{35}$$

If Q_m is high, B_{in} could be approximated as $\frac{\omega_s CC_0}{C+C_0}$ and equation (33) is reduced to equation (22). Equation (22) is also for illustrative purpose because α is an integer in that case and the non-ideal inductor effect is easier to understand.

4.4 Relation between Gain and Quality Factor

In Figure (29), the quality factor Q of the whole network is:

$$Q = \frac{R_{in}}{\omega_s L} \tag{36}$$

For simplification, it is assumed that Q_m is high here.

$$Q = R_{in} B_{in} \approx \omega_s R_m C_0 (1 + \frac{C_0}{C}) \tag{37}$$

Small C results in large R_{in}, large L, large voltage gain and large Q.

4.5 General Approach for Voltage Amplification

In general, resonance matching could be realized by configuration in either Figure 25 or Figure 26 for any pMUT, assuming the input impedance of the LNA is infinite.

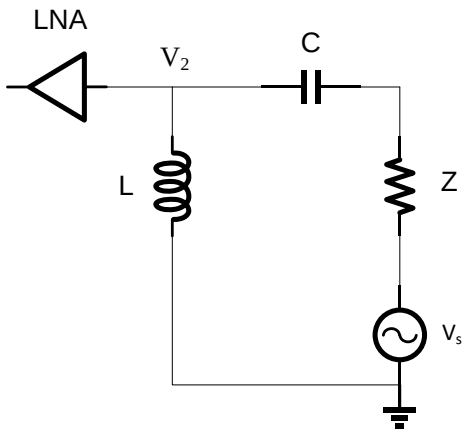

Figure 25. Configuration 1 for voltage amplification

$$\alpha = \frac{V_2}{V_s} = \frac{j\omega_s L}{j\omega_s L + \frac{1}{j\omega_s C} + Z} \tag{38}$$

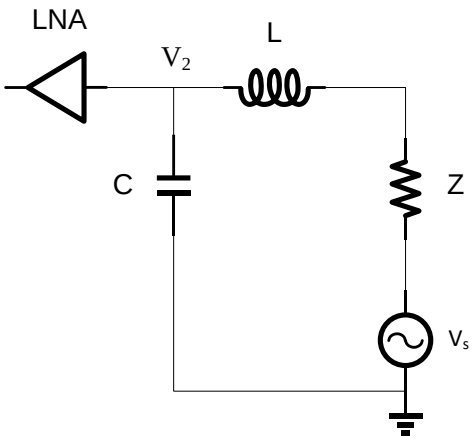

Figure 26. Configuration 2 for voltage amplification

$$\alpha = \frac{V_2}{V_s} = \frac{\frac{1}{j\omega_s C}}{j\omega_s L + \frac{1}{j\omega_s C} + Z} \tag{39}$$

Z could be complex impedance. For maximum voltage amplification, the total equivalent inductance will resonate with the total equivalent capacitance, giving resistive transformed impedance.

4.6 NF Reduction

The matching network can also reduce NF of the ultrasound system. The signal flow is shown in Figure 27. The ultrasonic wave is received by the transducer and converted into electrical signal, which feeds into LNA through the matching network. It should be noted that the voltage

amplification and NF reduction is realized only when receiving signals. $\overline{v_s^2}$ is the output noise of ultrasound transducer. $\overline{v_n^2}$ and $\overline{i_n^2}$ represent the input-referred noise of LNA. The passive network is assumed to be noiseless.

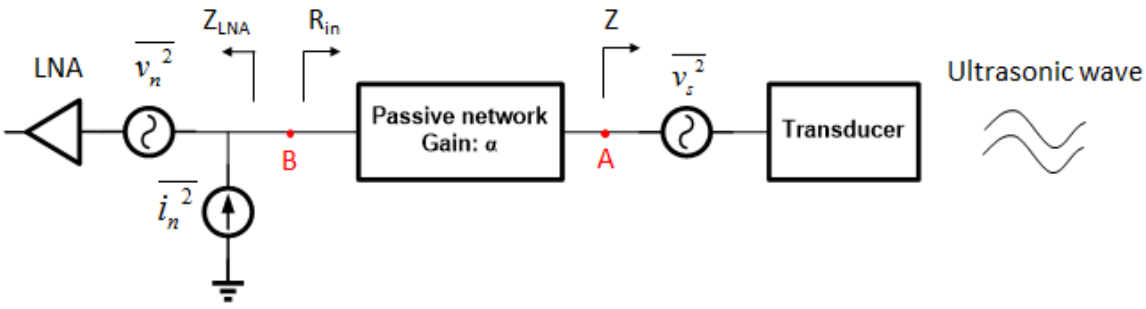

Figure 27. Front-end of ultrasound imaging system

The NF could be calculated by referring all noise parts to node B.

$$NF \approx 10\log(1+\frac{\overline{v_n^2}}{\overline{v_s^2}\,|\alpha|^2}) \tag{40}$$

Since the LNA is a CS amplifier with very high input impedance, $\overline{v_n^2}$ is much larger than $\overline{i_n^2}$. When $\overline{v_n^2} \gg \overline{i_n^2}R_{in}^2$, increasing $|\alpha|$ can reduce NF and this is why the resonance matching is used. As explained before, the matching network is an impedance transformer. R_{in} increases as $|\alpha|$ increases. When R_{in} is large enough, the current noise can no longer be ignored. Further increase in R_{in} will make the current noise dominate and NF will start to increase. There is an optimal value of R_{in} which results in the minimum NF.

Input impedance Z_{LNA} will not affect the NF. Actually $|\alpha|$ is considered as the gain of the independent stage without the loading effect of Z_{LNA}. Simply speaking, $|\alpha|$ is the gain of

matching network itself and it has no relation with Z_{LNA}. The loading effect is eliminated since it appears in both numerator and denominator. Z_{LNA} is desired to be large just for large input voltage.

4.7 Tunable Matching

The matching network could be made tunable as Figure 28. C_1 and L_1 form a tunable inductance L. Voltage gain is controlled by C. C_1 is tuned accordingly to make it resonate at the same operating frequency. For a given transducer, it provides the function of tunable gain. For a given LNA, different transducers could be catered at different operating frequencies.

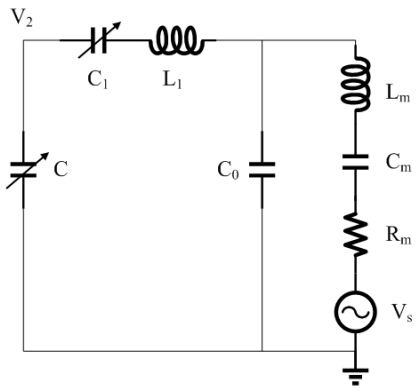

Figure 28. Tunable Matching

4.8 Wideband Matching

Ultrasound transducers are usually wideband devices and the matching network should maintain the bandwidth as well. Previous contents are just presented to explain the fundamental

theories of this matching technique. For real applications, the design method is more complicated. Adding one inductor and one capacitor is definitely not enough to realize wideband properties. Instead, multi-order structure should be used.

The initial impedance of pMUT should be measured first. Then the desired voltage gain will be used to calculate the desired impedance that should be raised to. Several inductors and capacitors are to be inserted to make the impedance transformation and the values of the passive components could be determined accordingly. Design steps and considerations are generalized as follows:

1. The desired impedance is calculated by multiplying initial impedance and square of desired voltage gain, which should still be 10 times smaller than the noise impedance of LNA and its input impedance.
2. Inductors and capacitors are inserted for impedance transformation. The number of those components are determined by the desired bandwidth. Wider bandwidth results in more components, higher noise and higher loss.

4.9 Comparison with Existing Matching Techniques

First of all, resonance matching is compared to 50Ω power matching. Power matching is also called impedance matching, which is aimed for maximum power transfer. The conventional RF design approach is to make Z_{LNA} to be 50Ω by feedback or source degeneration. The voltage at LNA's input is low because its input impedance is low.

Resonance matching aims to get large voltage at LNA's input. In Figure 29, V_1 is the voltage at LNA's input and V_2 is defined as the open terminal voltage at the output of passive network. The passive network is assumed to be lossless.

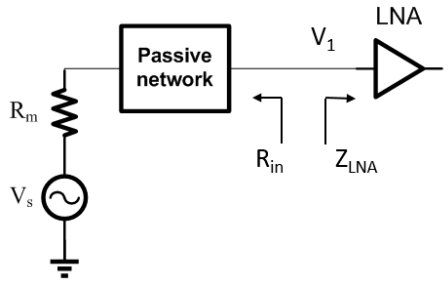

Figure 29. Illustration for Maximum Input Voltage

$$P = \frac{V_s^2}{R_m} = \frac{V_2^2}{R_{in}} \tag{41}$$

$$V_1 = V_2 \frac{Z_{LNA}}{Z_{LNA} + R_{in}} = \sqrt{PR_{in}} \frac{Z_{LNA}}{Z_{LNA} + R_{in}} \tag{42}$$

For a given source and given LNA, P and Z_{LNA} are known and R_{in} is the only variable. By taking derivative of equation (42), V_1 is maximized when R_{in}=Z_{LNA}. In this case:

$$V_1 = \frac{\sqrt{PR_{in}}}{2} = \frac{\sqrt{PZ_{LNA}}}{2} \tag{43}$$

This leads to the conclusion that Z_{LNA} should be large for large V_1, and V_{1max} is achieved when impedance is matched. High impedance matching is just the special case of resonance matching in which V_1 is maximized. In reality, Z_{LNA} is capacitive. Matching the source resistance with the capacitance through LC network is not feasible. Therefore RF designers have to modify the structure of LNA to get 50Ω for maximum power transfer. For ultrasound imaging system,

large voltage signal is wanted so high input impedance LNA is used. Resonance matching can produce a much larger input voltage than 50Ω design.

When compared to noise matching, resonance matching has certain advantages. As explained before, noise matching may require a very large inductor which is not practical to implement. Besides, the voltage gain provided by resonance matching is favorable and this gain could be set by the designer, which noise matching could not guarantee.

There seems to be certain similarities between resonance matching and passive amplification, but when scrutinizing the theories, the differences are apparent. Passive amplification is proposed for antenna and coil whose structures are totally different from ultrasound transducer. The second-order filter structure of passive amplification is not applicable to ultrasound transducer. More importantly, passive amplification is based on making one inductor and one capacitor at resonance but the invented method is founded on impedance transformation through multi-order structure. Also, there are co-design considerations between matching network, transducer and LNA in resonance matching instead of just making two components at resonance.

To conclude, resonance matching is different from power matching, noise matching or passive amplification because the methodology behind is totally different. Resonance matching is specially invented for pMUT and its benefit will be shown in Chapter 5.

Power matching is not applicable to ultrasound system because the input impedance of LNA is much higher that of pMUT. Working frequency of pMUT is normally below 20MHz and the

input impedance of ultrasound LNA is usually several hundred kΩ while the magnitude of the pMUT impedance is typically a few hundred Ω. Noise matching is also not feasible because it may require a large inductor of several mH for matching and the inductor will cause large loss and noise. Besides, noise matching may not be able to provide the voltage gain. Passive amplification reported in the literature is not applicable to pMUT because that structure could not provide any voltage gain, which could be seen from the previous derivation.

Chapter 5 Results and Discussion

The current situation is that, for ultrasound imaging system, people either use a 50Ω LNA and power matching, or a high input impedance LNA without any matching like the common analog circuit. As explained before, the input voltage is halved if 50Ω LNA is used, which is not wanted in ultrasound design. As for using high input impedance LNA, resonance matching will provide extra voltage gain and NF reduction compared to the no matching situation. Thus, the comparison of results are made between these two situations: a high input impedance LNA with resonance matching and the same LNA without matching. Other matching techniques are not applicable when a high input impedance LNA is used, which has already been clarified in the literature review and Chapter 4.9.

In this chapter, experiments and simulations are conducted to verify that resonance matching can provide voltage amplification and NF reduction. Results have shown there is over 15dB gain and 6dB SNR improvement by adopting this matching technique. Standard testing

procedures for the ultrasound transducer are defined by American national standard E1065 and shown in Figure 30.

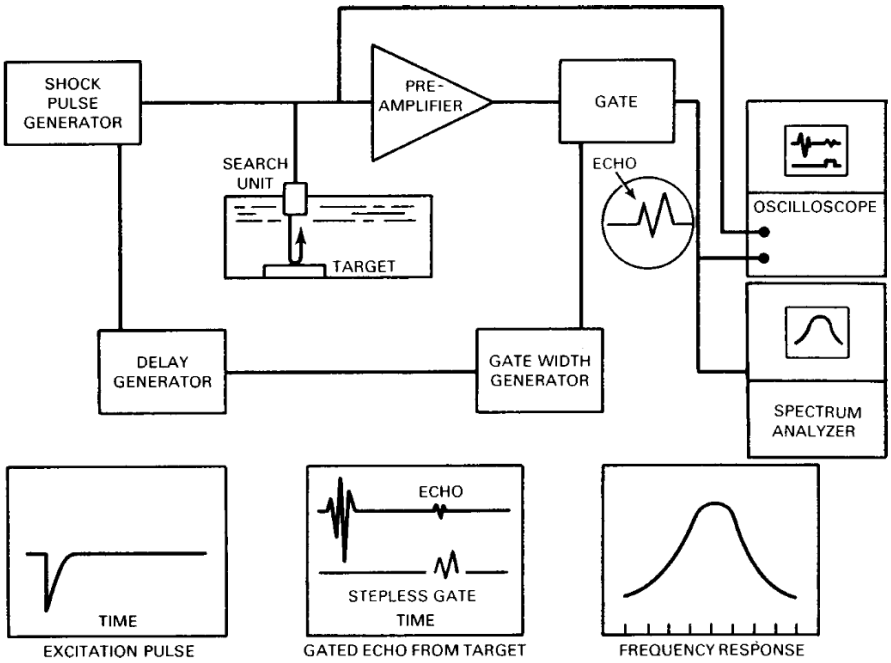

Figure 30. Shock excitation method for ultrasound transducer measurement

5.1 Testing Results of Narrow Band Matching

As explained before, resonance matching is applied only in the receiving path. Thus the experiment setup is modified a bit as Figure 31. Narrow band matching is first performed to demonstrate the theory and expose some interesting problems.

Pulses are generated by the shock pulse generator to excite transducers. Two identical transducers are used. One is for transmitting (Tx) and the other is for receiving (Rx). They are completely immerged in a water tank. The distance between the transducers are different from

the standard due to limitation in lab environment. However, it is not an issue as long as the distance is fixed during comparison. Resonance matching network including a 4.7μH inductor and a 56pF capacitor is used. An oscilloscope with 1MΩ input impedance is used to collect data. Devices are connected through RG-58 cables with 50Ω characteristic impedance. The data is then put into Matlab for processing.

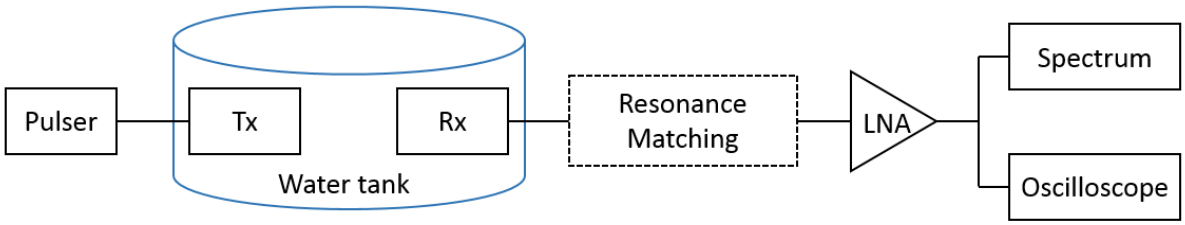

Figure 31. Experiment setup for verification of voltage amplification

Signals in time domain are shown in Figure 32 and the frequency information is shown in Figure 33. It could be seen clearly that amplitude of the signal is amplified after resonance matching. It is found that the transducer actually works at 8.5MHz. In Figure 33, the peak with matching network is at 6.5MHz, which is much smaller than the designed operating frequency due to the transmission line (TL) effect.

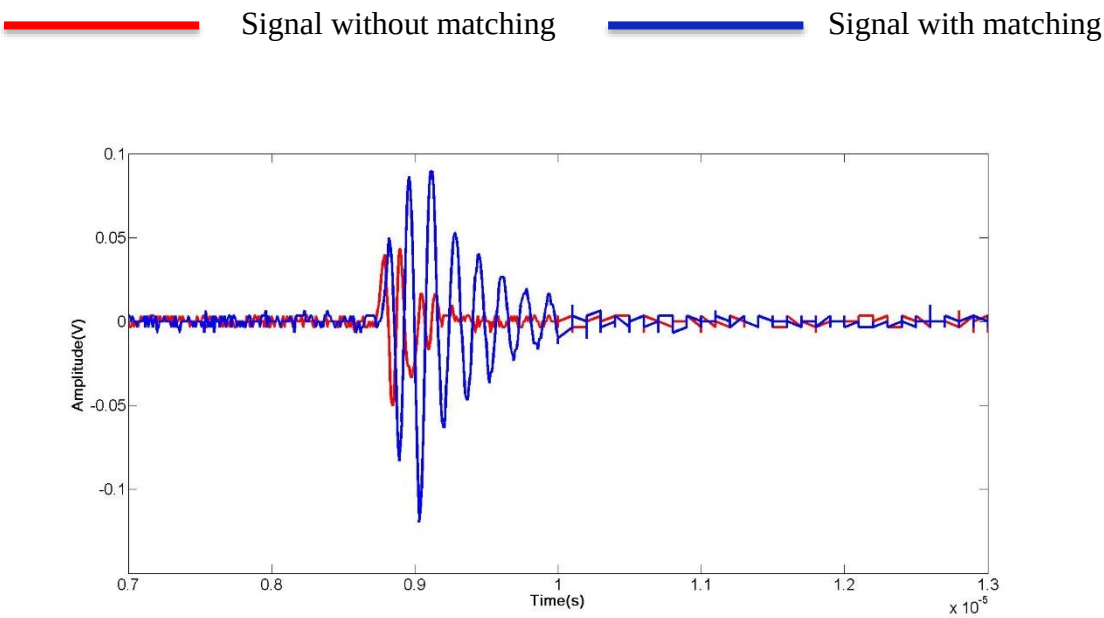

Figure 32. Comparison of signals with and without matching in time domain

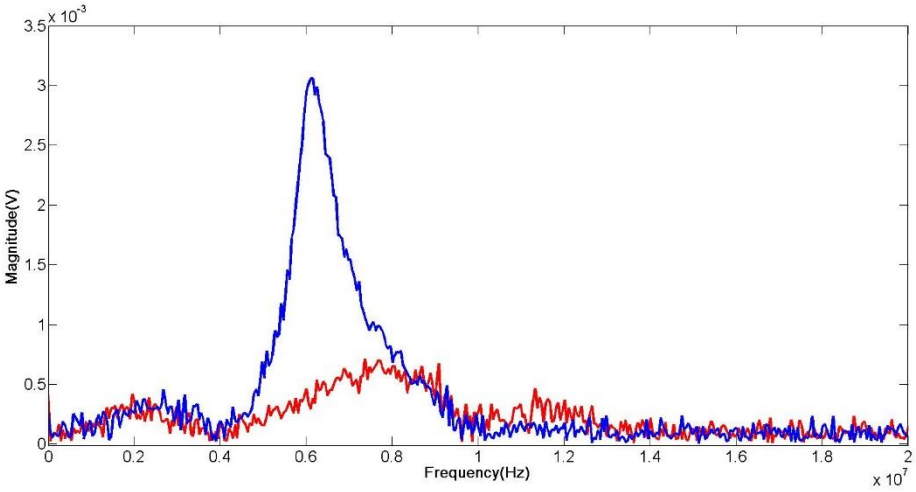

Figure 33. Comparison of signals with and without matching in frequency domain

Transmission Line Effect

The coaxial cable used in the experiment is about 46cm. The operating frequency is low and

the transmission line effect needs to be considered. The input impedance of LNA is quite high. After adding the transmission line, its impedance rotates clockwise along the smith chart referring to the center point as shown in Figure 34. The impedance becomes capacitive which makes the total capacitance larger and the actual peak frequency smaller.

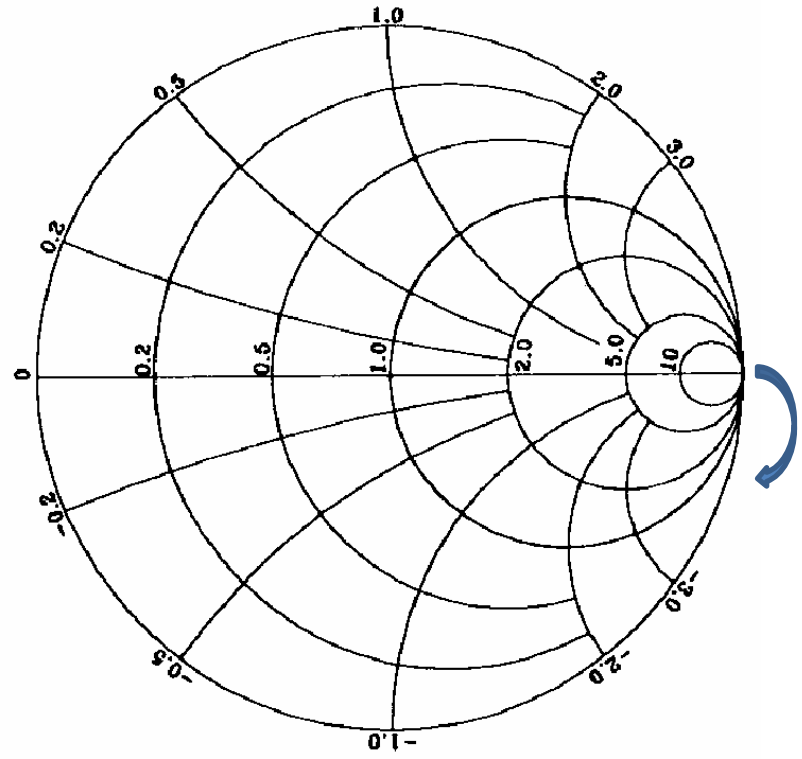

Figure 34. Transmission line introduces an equivalent capacitor

The impedance Z_{in} looking into the LNA with a TL is:

$$Z_{in} = Z_0 \frac{Z_L + jZ_0 \tan(\beta l)}{Z_0 + jZ_L \tan(\beta l)} \tag{44}$$

Z_0 is 50Ω, Z_L is 1MΩ and βl=8degree when l=46cm. Z_{in}=0.916-j356.336(Ω) which is equivalent to a 0.916Ω resistor in parallel with a 45pF capacitor. This capacitor results in the peak frequency shift.

This is quite different from the conventional 50Ω design. If each impedance is 50Ω, adding TL only rotates the 50Ω impedance point around the center point which also represents 50Ω. That means no matter how long the TL is, the impedance is still 50Ω. However, for resonance matching, the input impedance of LNA is high for large input voltage. There are two ways to eliminate TL effect. One way is trying to use short line but it is not effective for discrete devices. If all things could be put into IC, there should be no problem. The other way is to use TL with length of λ/2 so that the TL can be ignored.

The experiment is conducted again after realizing TL effect. Another TL is used and value of *C* is adjusted to make peak frequency at 8.5MHz. The improved results are shown in Figure 35 and Figure 36. From Figure 36, it can be observed that the peak frequency is at 8.5MHz as wanted and voltage gain of 20dB is achieved.

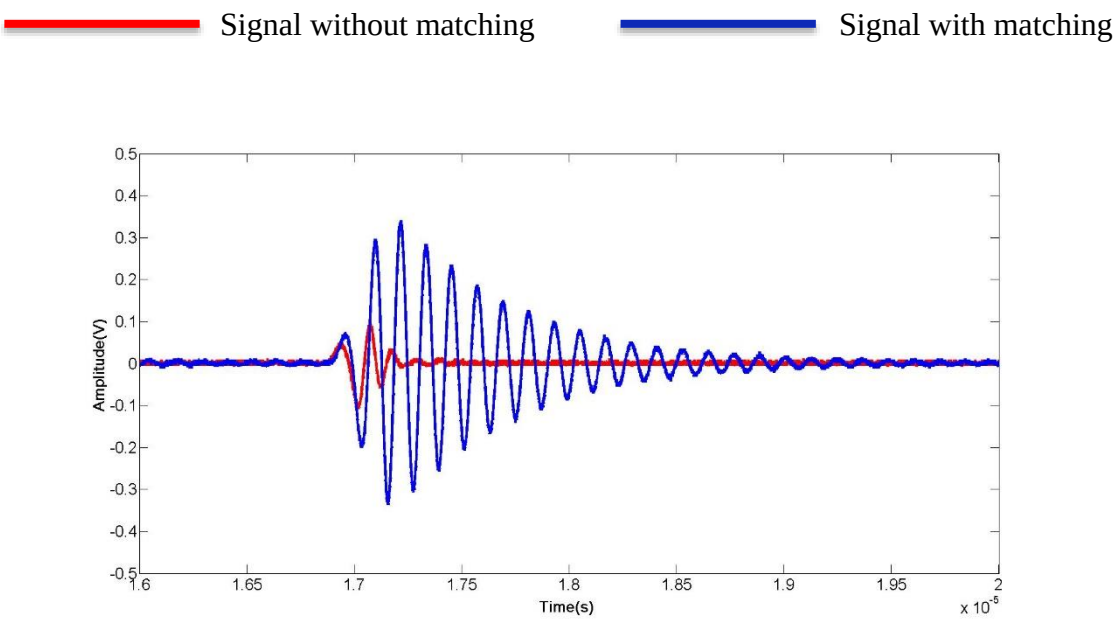

Figure 35. Comparison of signals with and without matching in time domain

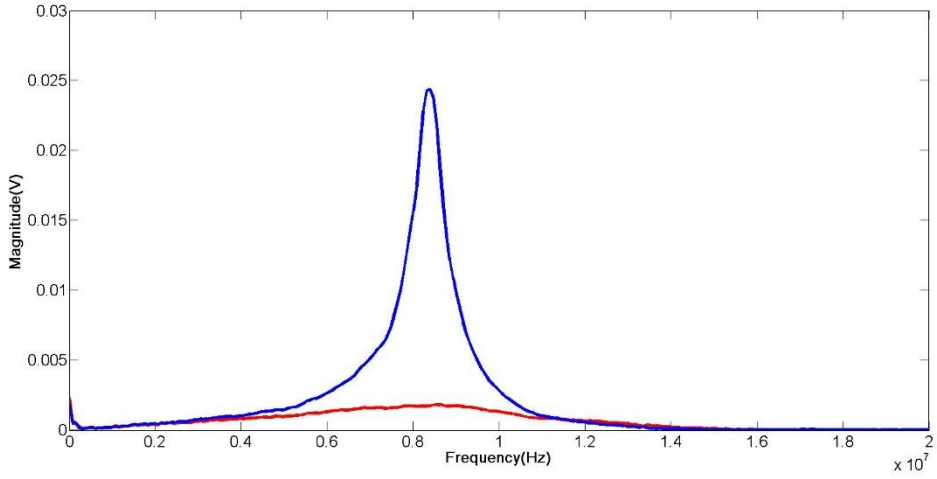

Figure 36. Comparison of signals with and without matching in frequency domain

Ringing Effect

Another interesting problem observed in above results is that the ringing of signal in time domain is quite significant. In Figure 35, signal without matching will die out after 0.5μs. After matching, signal will die out after 2μs instead. This ringing effect will reduce the resolution of ultrasound imaging system because the reflected signals from two adjacent points will overlap.

This ringing effect is caused by the sharp roll-off of the matching network in frequency domain. Passive amplification suffers from this effect but resonance matching is able to overcome it by using multi-order structure for wideband matching.

5.2 Results of Wideband Matching

Simulation Results

As explained before, most ultrasound transducers are wideband devices and some even have fractional bandwidth over 50%. Several inductors and capacitors have to be used for resonance matching. Simulations are performed in ADS as Figure 37. The pMUT block is the electrical model of a commercial transducer whose operating frequency is 8.5MHz with 60% fractional bandwidth. The frequency response of transducer is measured and shown in Figure 39. The 1mV signal source simulates the signal received by this pMUT. A multi-order network is used for matching and inductors are non-ideal in simulation. The voltage gain is designed to be 8 and it is required to maintain the bandwidth of pMUT. LNA is represented by its PSPICE model with resistor feedback, providing 26dB gain.

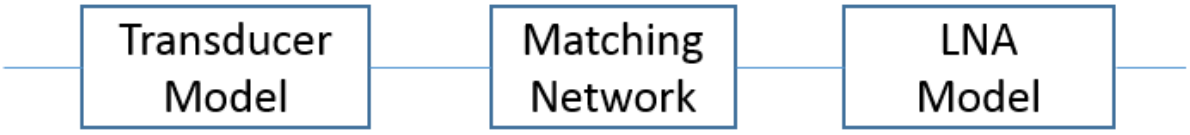

Figure 37. Wideband matching simulation

Results are plot in Figure 38. In Figure 38, signal with matching at 8.5MHz is -29dB. Signal without matching is about -46dB and voltage gain is 17dB. For voltage plot, the bandwidth is cut off at -6dB point. It could be seen that wideband matching is achieved with a gain over 15dB across the bandwidth from 6.5MHz to 11MHz.

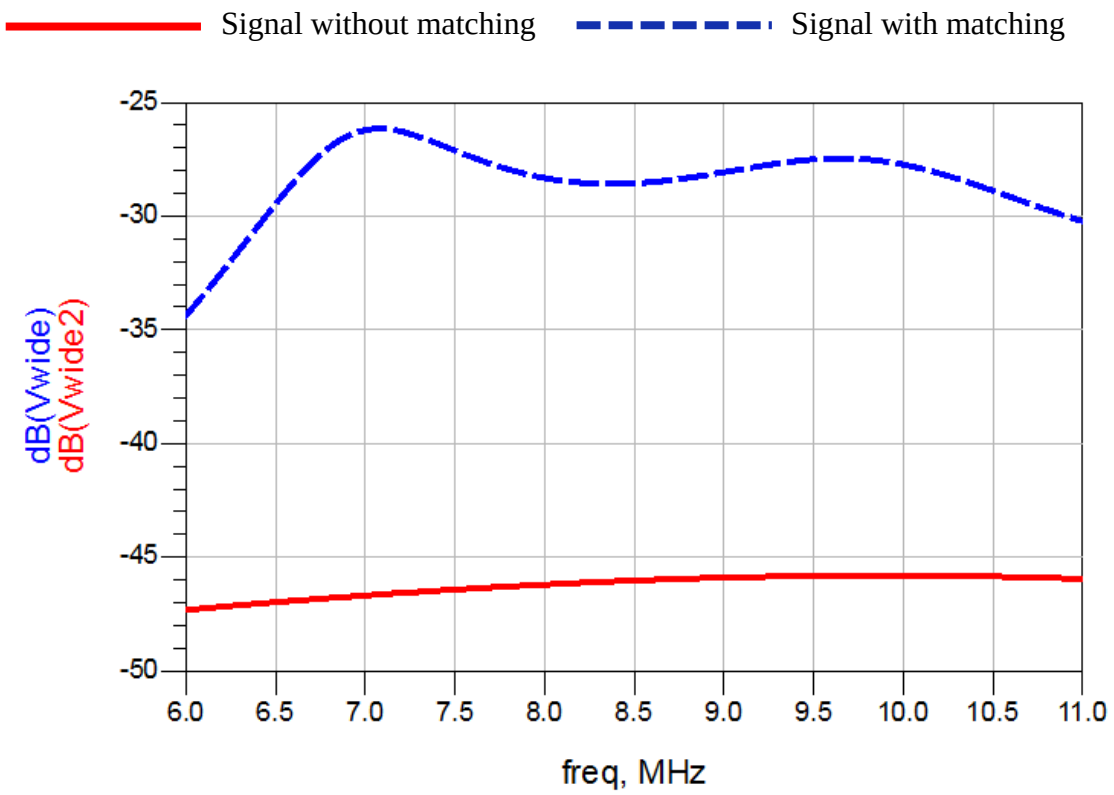

Figure 38. Simulation results with and without matching in frequency domain

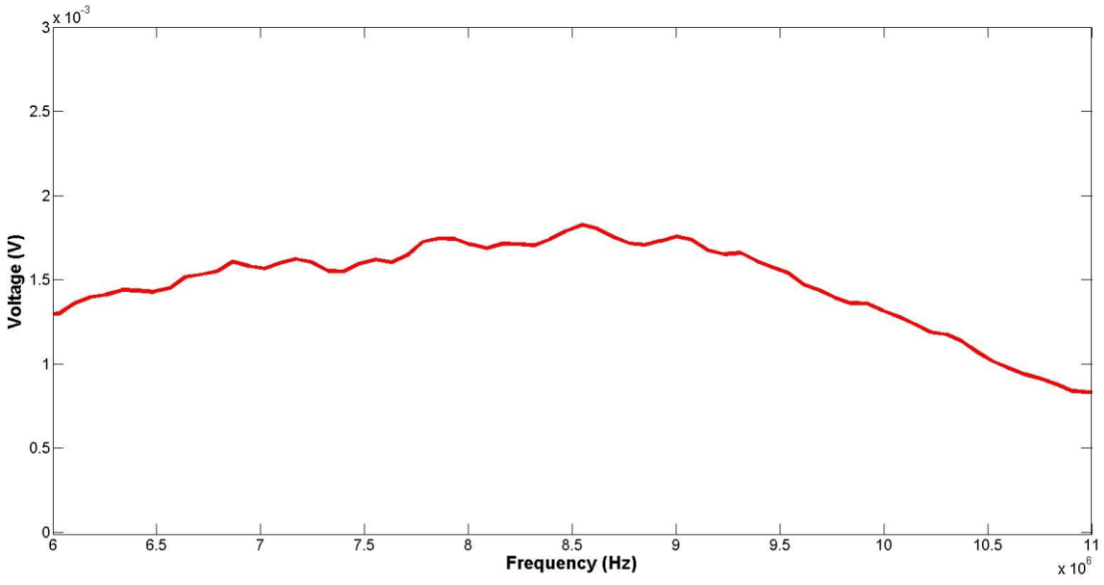

Figure 39. Measured frequency response of the transducer

Time domain signals are also simulated to prove the effectiveness of resonance matching. The

pulser is represented by a pulse voltage source, the transducer model extracted in Chapter 3 is used here, and the matching network consists of 2-stage LC ladders. Simulation results are shown in Figure 40.

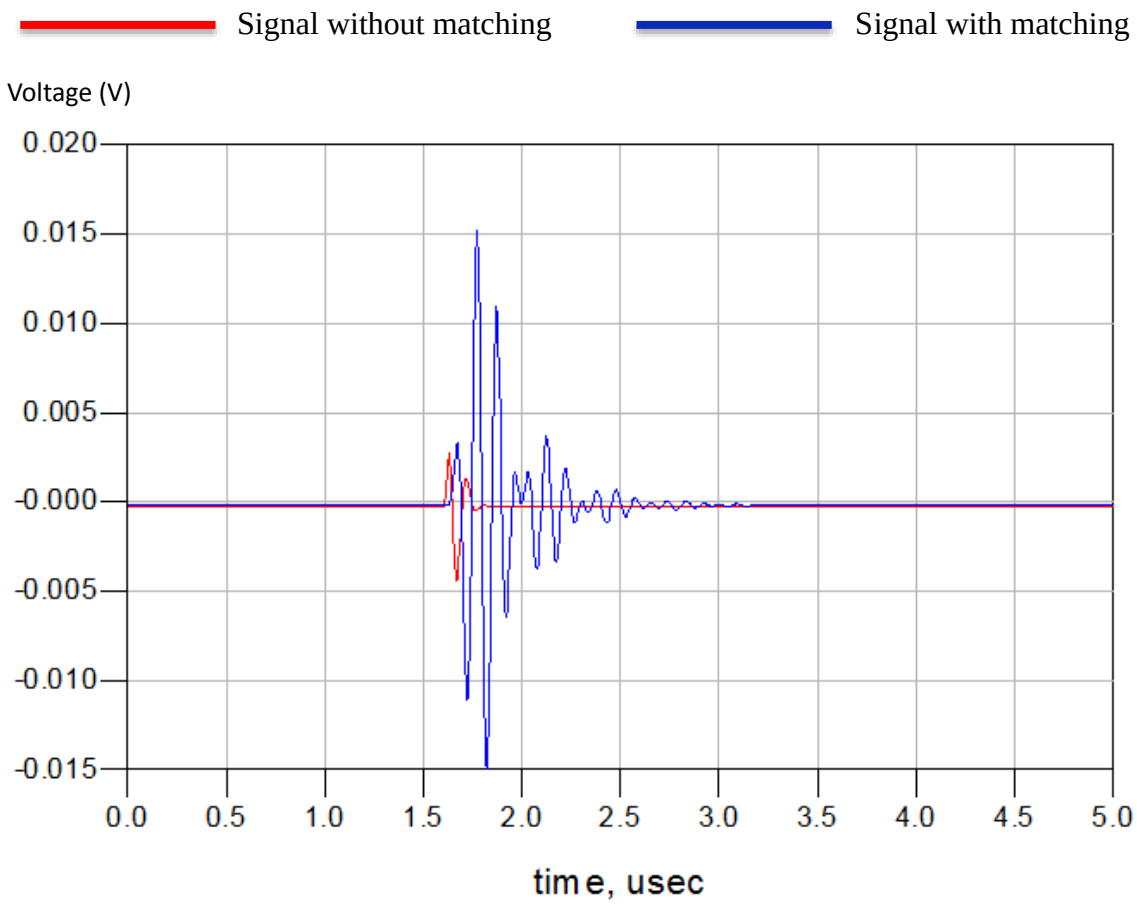

Figure 40. Simulation of time domain signal

When compared to the testing results in the Figure 41, it could be seen that the waveforms are very similar, proving that the modeling of transducer is accurate. The peak-to-peak values of the time domain signals are close to the testing results as well as the width of signals along horizontal axis. The loss of acoustic transmission and conversion is considered in simulation and modeled by conversion efficiency. One thing needs to be clarified is that the delay along

horizontal axis is different. It is because there are two transducers and the delay of receiving could not be accurately represented in simulation. However, this is not an issue as long as the waveforms are simulated correctly. The results indicate resonance matching can provide significant voltage gain as predicted.

Testing Results

A PCB has been made and tested using setup in Figure 31. The results of time domain signal are shown in Figure 41. The voltage gain is about 14dB which is consistent with the simulation results. Compared to the previous narrow band matching, the ringing effect is significantly reduced. Though there is still some ringing, it is due to introducing another stage. The bandwidth in frequency domain of matching network is designed to match the bandwidth of transducer and inevitably, time domain response is broadened.

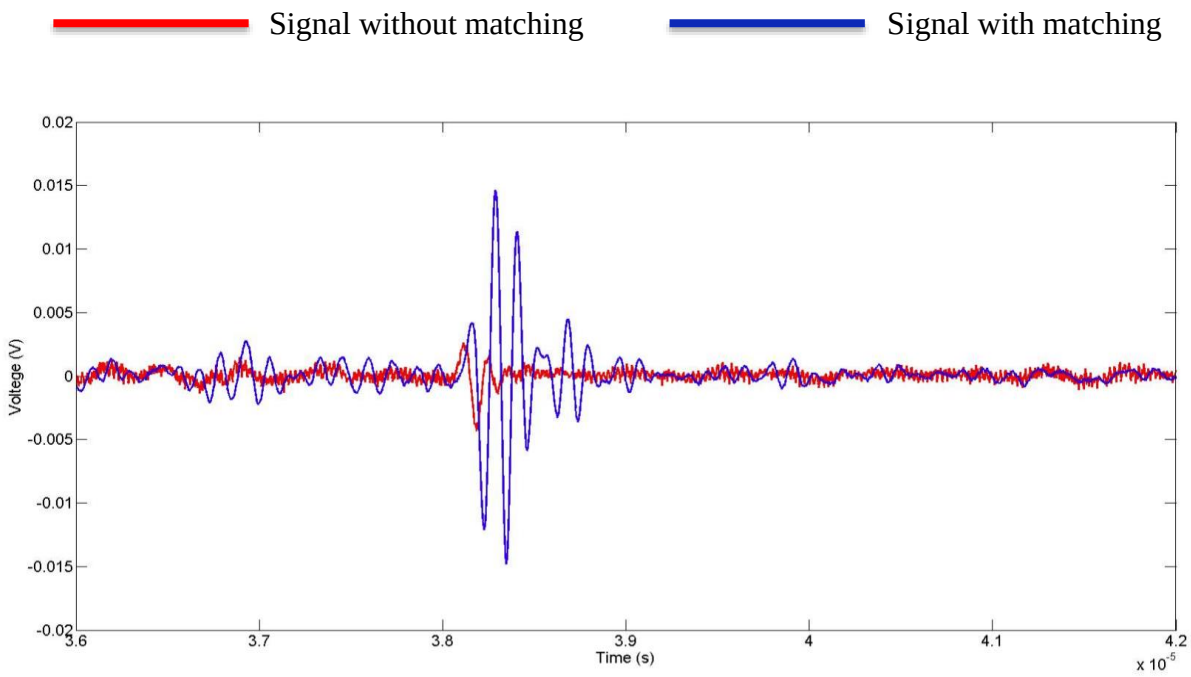

Figure 41. Time domain signals with and without matching for wideband transducer

The frequency response is shown in Figure 42 which is obtained by substituting the pulser with a sine source and sweeping the frequency across the bandwidth of transducer. Results are displayed on spectrum analyzer. It could be observed that there is about 14dB gain over the bandwidth.

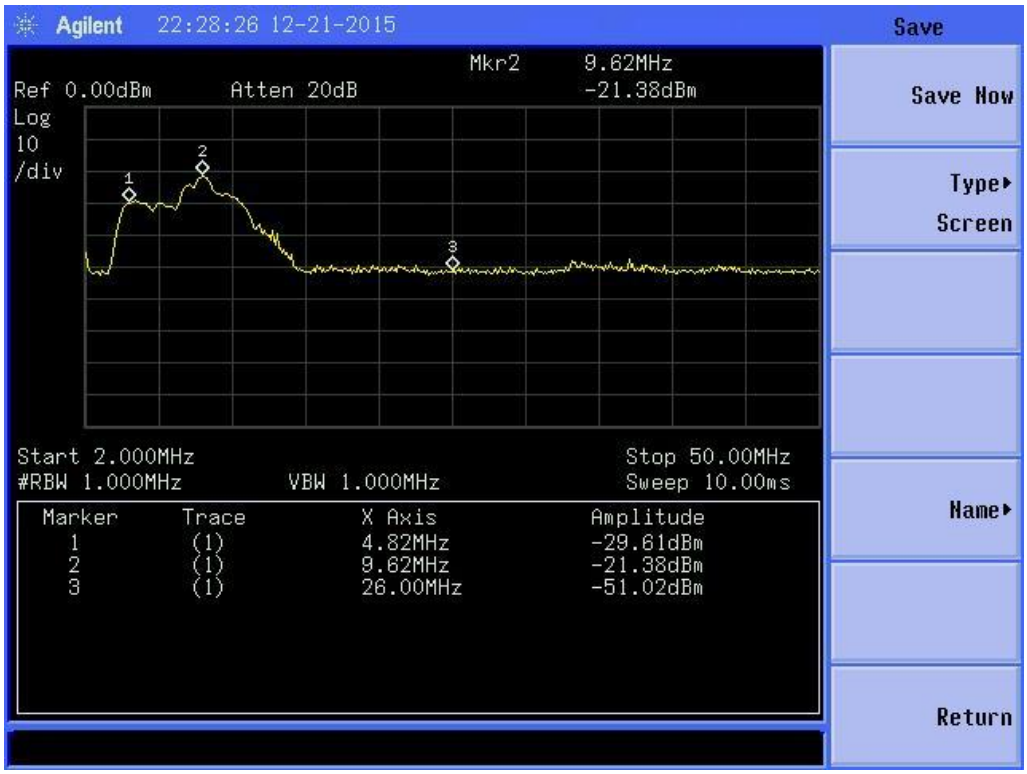

Figure 42 (a). Frequency response without matching

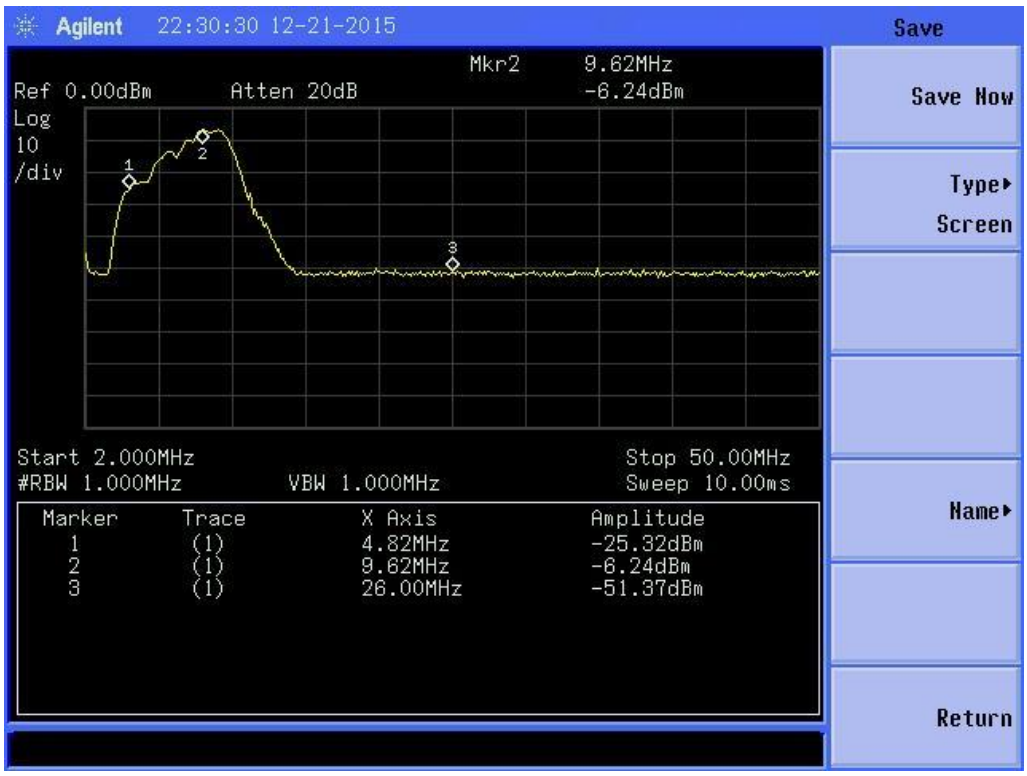

Figure 42 (b). Frequency response with matching

The reason of using sine source instead of pulser is that the pulser will transmit pulse train at certain frequency and the spectrum analyzer could not capture a steady signal. Therefore the signal spectrum looks a bit different from Figure 43 because data in Figure 43 is obtained by doing FFT of time domain signal with a pulser as input. There are some systematical errors of the equipment. Another point needs to be clarified is that the input impedance of spectrum analyzer is fixed to be 50Ω, thus the power gain is of the same number as the voltage gain in dB.

SNR Improvement

NF of the system could not be measured directly since ultrasound transducer is a one-port device. However, it could be represented in terms of SNR. NF reduction means the increase in SNR. Resonance matching will amplify source noise in the bandwidth but output SNR will still increase. Noise floor of the system is measured without any input. Total noise power in the bandwidth is integrated and represented as channel power in Figure 43. Noise floor is raised by 8dB within the bandwidth while signal is amplified by 14dB, resulting in 6dB improvement in output SNR.

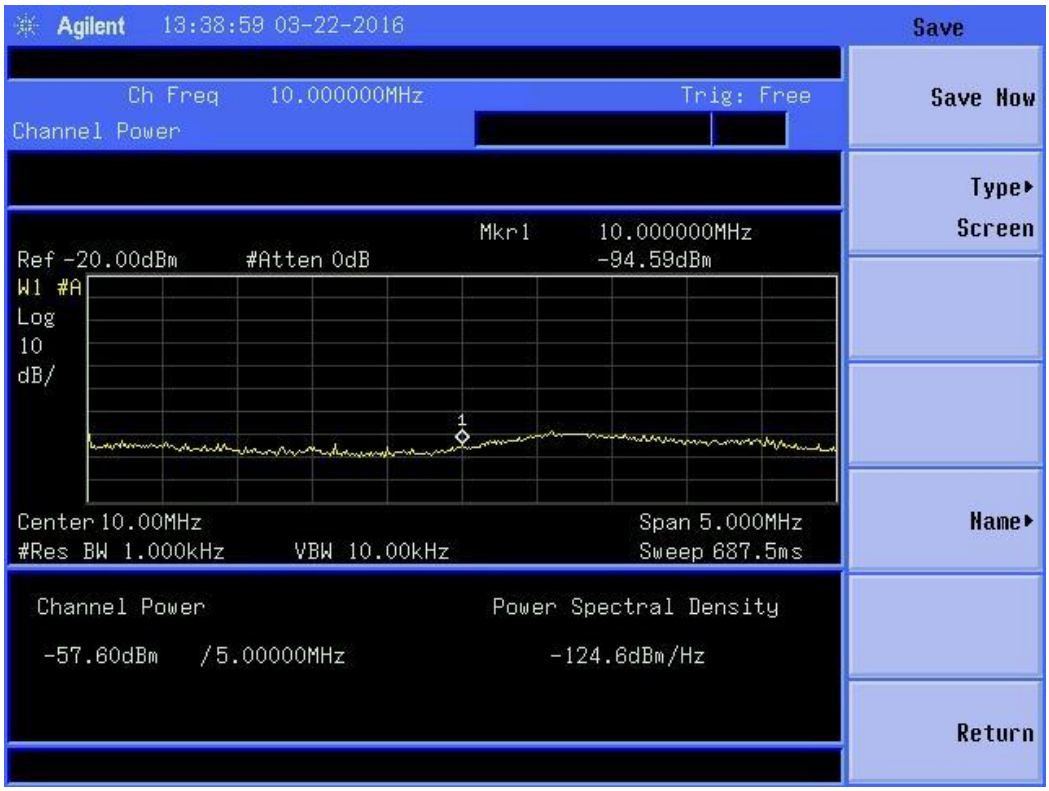

Figure 43 (a). Noise floor in band with matching

Figure 43 (b). Noise floor in band without matching

Compensation for Frequency Response

Resonance matching has another advantage of compensating the imperfect frequency response of ultrasound transducer. The frequency responses of some transducers are not very flat within the bandwidth. One example is shown in Figure 44 which is captured from the datasheet of a commercial product. The in-band ripple is large and it is not symmetrical. By adding resonance matching network, the total frequency response could be compensated. The ripple could be reduced by inserting poles at proper positions. Testing results of this advantage are shown in Figure 45. It is clear that the frequency response is flatter and more symmetrical after applying resonance matching.

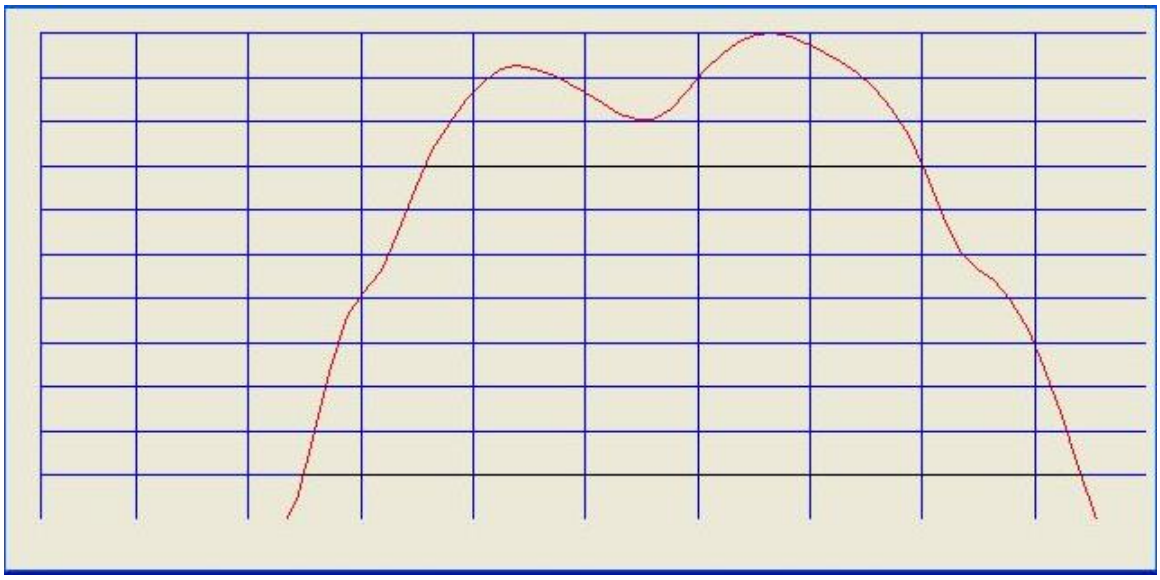

Figure 44. An example of imperfect frequency response

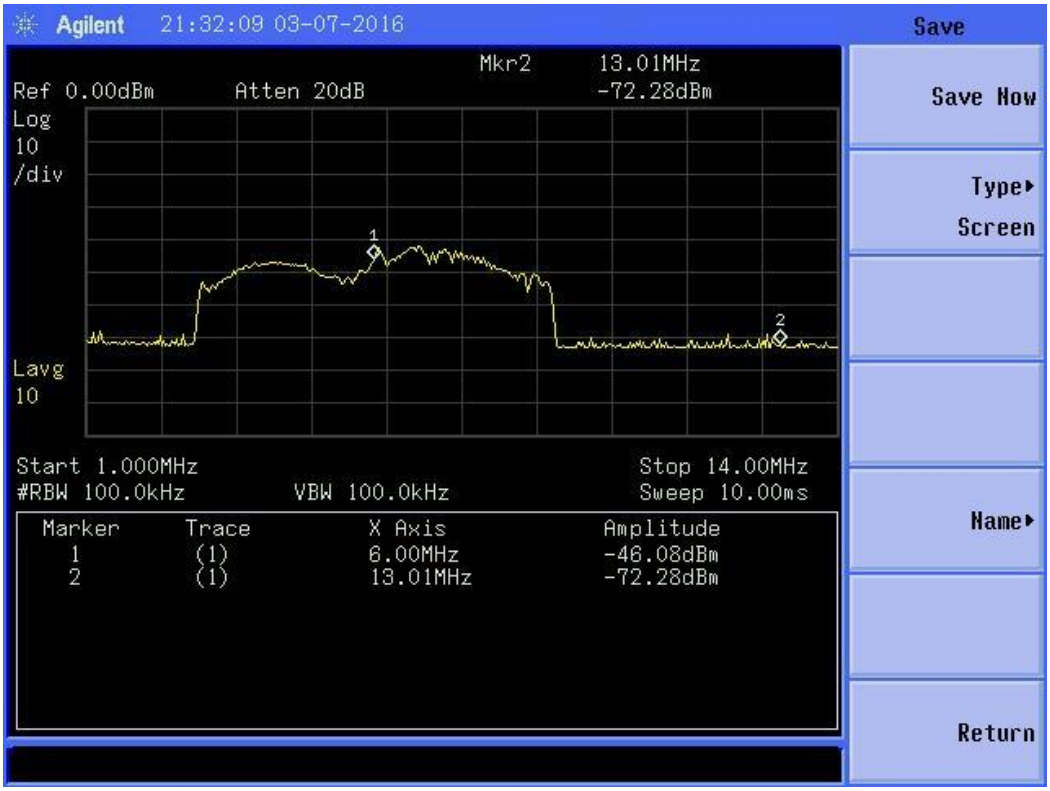

Figure 45 (a). Measured frequency response without matching

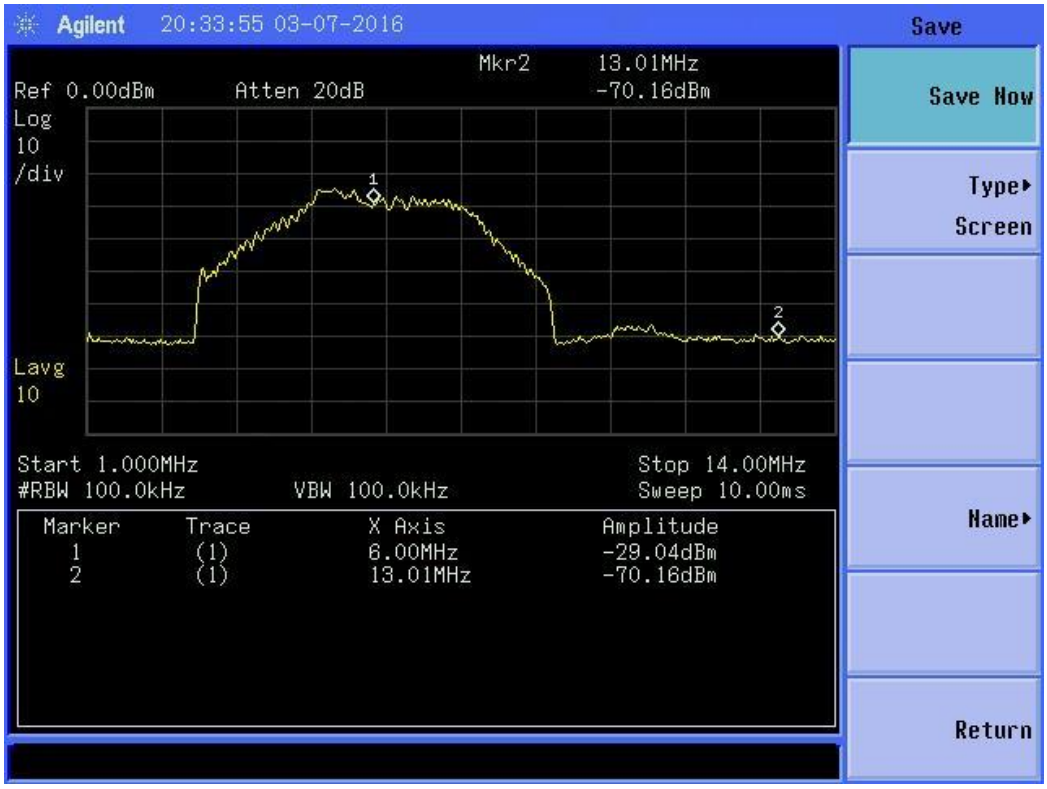

Figure 45 (b). Measured frequency response with matching

5.3 Testing Results of Improved Sensitivity

Sensitivity of the system is defined as the minimum input signal that could be detected. Experiments are designed to show that resonance matching can improve sensitivity of the system. A pMUT is put in a water tank to detect a target. The echo is amplified by LNA and measured in oscilloscope. The distance *d* from pMUT to target is a measure of sensitivity. Longer distance results in smaller amplitude of the echo. If the system could detect the target at further distance by adding resonance matching network, it means the sensitivity is improved.

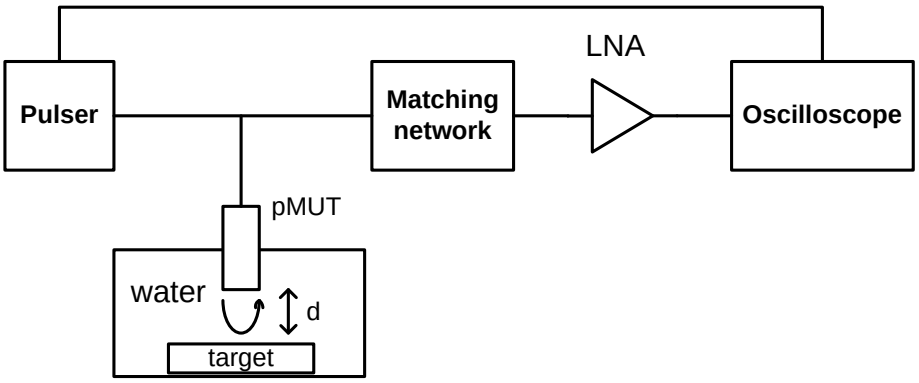

Figure 46. Experiment setup for testing the improved sensitivity

Results are shown in Figure 47 and Figure 48. When *d* is increased to 35mm, without resonance matching, we could not observe any useful signal in Figure 47. The echo is shadowed by noise. It means this system is limited to detect targets at maximum distance of 35mm.

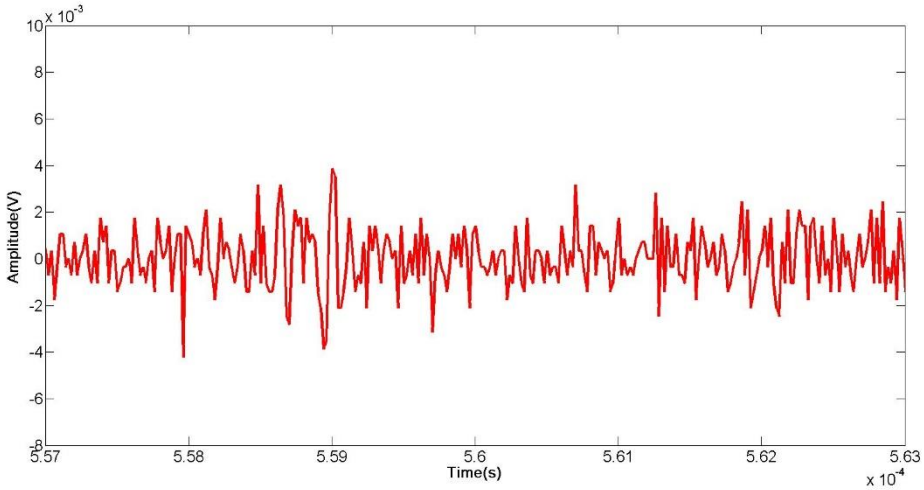

Figure 47. Received signal without resonance matching

By using resonance matching, when *d*=35mm, we could clearly see the echo in Figure 48 indicated by the circle. When *d* is further increased to 40mm, we start to get the similar results as Figure 47. It demonstrates that with resonance matching network, the maximum distance of

detection is increased from 35mm to 40mm, meaning the sensitivity of the system is improved.

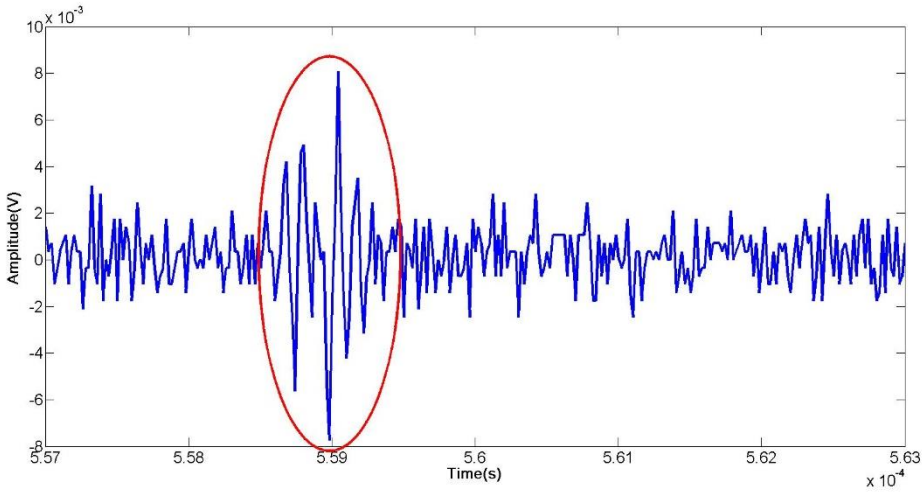

Figure 48. Received signal with resonance matching

Chapter 6 LNA Design

A typical differential amplifier is designed for ultrasound imaging system and the primary concern is the input-referred noise. The LNA structure is shown in Figure 49 which is founded on 0.18μm CMOS technology. The input transistor should have large g_m while the load transistor should have small g_m for low input-referred noise. The DC bias current is wanted to be large to get large g_m for the input transistor. Cascode is used for gain boosting without injecting noise. Common mode feedback by using two large resistors is used for low noise. The simulated input-referred noise is $0.9\text{nV}/\sqrt{\text{Hz}}$ at 8.5MHz.

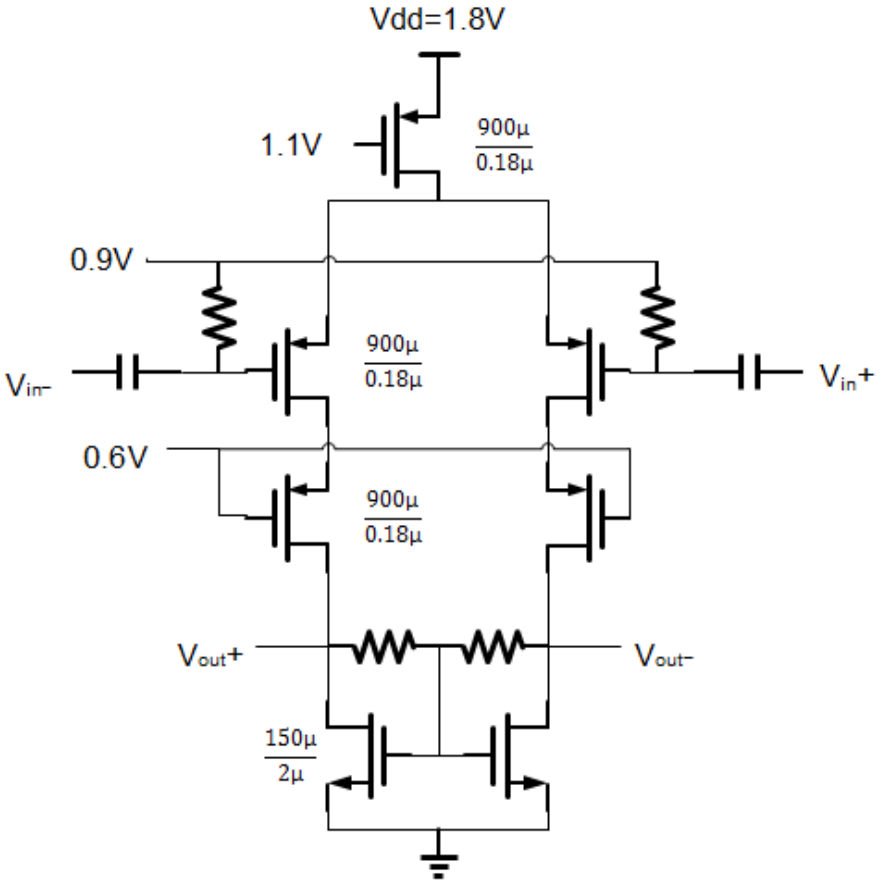

Figure 49. LNA structure

The LNA is just used to illustrate the co-design considerations of resonance matching. The input impedance of LNA should be high in order to have large input voltage. The only concern of LNA design is to get low input-referred noise. Some specifications are listed in Table 5.

Voltage gain	Output impedance	Bandwidth	Input noise at 8.5MHz	Input impedance	Current
40dB	50Ω	15MHz	$0.9nV/\sqrt{Hz}$	100KΩ	8.8mA

Table 5. Specifications of LNA

Comparisons are made with other two ultrasound designs that adopt the similar high input impedance LNA structure.

	This work	[14]	[15]
Voltage gain	40dB	41dB	20dB
Noise performance	$0.9\text{nV}/\sqrt{\text{Hz}}$ simulated at 8.5MHz	$1.8\text{nV}/\sqrt{\text{Hz}}$ measured at 21.3MHz	10dB NF

Table 6. Comparison of noise performance with other ultrasound LNA

The noise performances of those LNA are comparable. The point is that by using resonance matching, the NF could be reduced significantly in such kind of design. Simulation results are provided below.

When the LNA is simulated with the ultrasound transducer model and the matching network, its NF reduces significantly as in Figure 50. The red line represents the NF without matching while the blue line represents NF with matching. At 8.5MHz, NF drops from 10dB to less than 1dB.

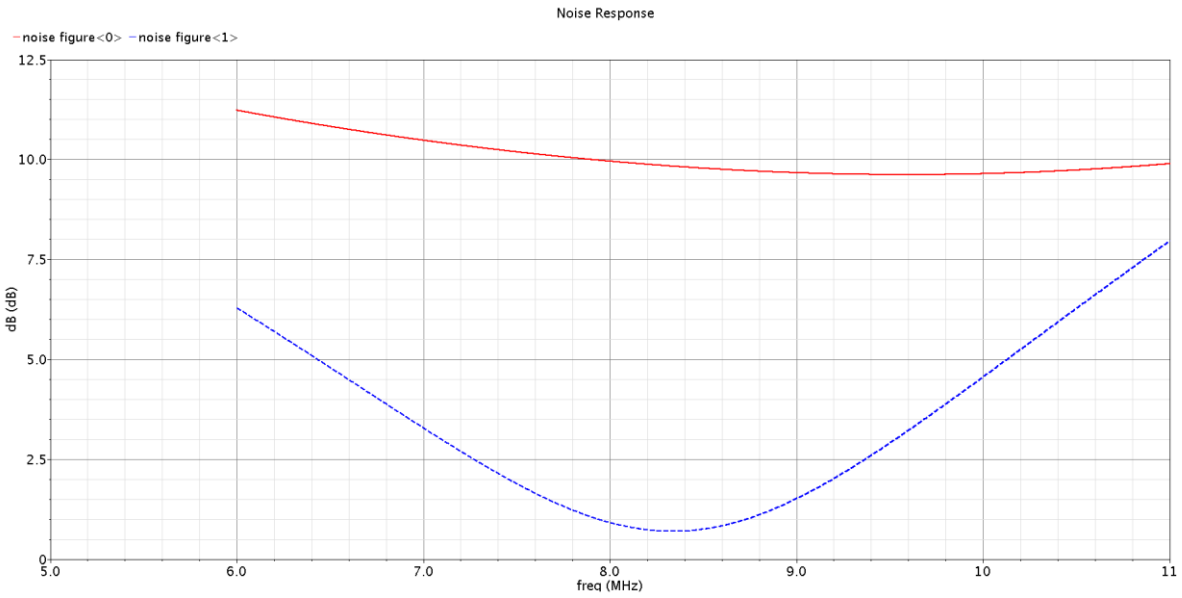

Figure 50. Comparison of NF with and without matching network

The reason to design a LNA here is to show that resonance matching can reduce NF of front-end significantly. As long as the LNA has high input impedance, using resonance matching for such ultrasound system is beneficial.

Chapter 7 Conclusion and Recommendation

The thesis has introduced a novel front-end receiver design for ultrasound imaging system by using resonance matching technique. The matching methodology is new and there are co-design considerations between pMUT, matching network and LNA.

Since the matching network is specially designed for pMUT, a systematical way of modeling pMUT is developed first. The author is the first one to report the detailed steps to calculate all electrical parameters of the general pMUT model especially when there is more than one

resonance. This method is simple and simulation and experiment results show than it is correct with 95% accuracy.

A new matching technique is invented which is totally different from RF power matching, noise matching or passive amplification. Resonance matching method is well explored which could be used for voltage amplification and NF reduction. Voltage gain of 15dB and SNR increase of 6dB is achieved indicating that sensitivity of the system has been improved a lot.

The designed LNA is simulated with resonance matching network to further prove the matching technique could reduce NF significantly. The input impedance of LNA should be high and the transistors should be sized properly to get low input-referred noise.

This invention has been patented through Singapore Patent Office.

In future, it is recommended to explore how to reduce the ringing effect. Adding the matching network will cause ringing which is not wanted in ultrasound imaging systems because the ringing will reduce resolution of the system. By using multi-stage matching network, this negative effect could be reduced a bit, but it is still not good enough. There is always trade-off between matching and ringing. The future work may focus on signal processing algorithm which can help minimize the ringing effect.

Bibliography

[1] S. Shelton, M. L. Chan, B. Boser, I. Izyumin, T. Frey, M. Judy, … K. Nunan, "CMOS-Compatible AlN Piezoelectric Micromachined Ultrasonic Transducers," *IEEE International Ultrasonics Symposium Proceedings*, vol. 10, pp. 1109, 2009.

[2] I. O. Wygant, M. Kupnik, J. C. Windsor, W. M. Wright, M. S. Wochner, G. G. Yaralioglu, M. F. Hamilton, and B. T. Khuri-Yakub, "50 kHz Capacitive Micromachined Ultrasonic Transducers for Generation of Highly Directional Sound with Parametric Arrays," *IEEE Trans. Ultrason. Ferroelectr. Freq. Control*, vol. 56, pp. 193-203, Jan 2009.

[3] O. Oralkan, A. Ergun, J. Johnson, M. Karaman, U. Demirci, K. Kaviani, T. Lee, and B. Khuri-Yakub, "Capacitive micromachined ultrasonic transducers: next-generation arrays for acoustic imaging?" *IEEE Trans. Ultrason., Ferroelectr., Freq. Control*, vol. 49, no. 11, pp. 1596 –1610,Nov. 2002.

[4] I. Wygant, M. Kupnik, J. Windsor, W. Wright, M. Wochner, G. Yaralioglu, M. Hamilton, and B. Khuri-Yakub, "50 kHz capacitive micromachined ultrasonic transducers for generation of highly directional sound with parametric arrays," *IEEE Trans. Ultrason., Ferroelectr., Freq. Control*, vol. 56, no. 1, pp. 193–203, Jan. 2009.

[5] V. Kaajakari, T. Mattila, A. Oja, and H. Seppa, "Nonlinear limits for single-crystal silicon microresonators," *J. Microelectromech. Syst*., vol. 13, no. 5, pp. 715 – 724, Oct. 2004.

[6] P. Fabijanski and R. Lagoda, "Modeling and Identification of Parameters the Piezoelectric Transducers in Ultrasonic Systems," *Advances in Ceramics - Electric and Magnetic Ceramics, Bioceramics, Ceramics and Environment*, Prof. Costas Sikalidis (Ed.), ISBN: 978-953-307-350-7, 2011

[7] S. Butterworth, “On a null method of testing vibration galvanometers,” *Proc. Phys. Soc. (London),* vol. 26, pp. 264–273, Dec. 1913–Aug. 1914.

[8] K. S. Van Dyke, “The electric network equivalent of a piezoelectric resonator,” *Phys. Rev.,* vol. 25, no. 6, p. 895, Jun. 1925.

[9] C. Kauczor and N. Frohleke, “Inverter topologies for ultrasonic piezoelectric transducers with high mechanical Q-factor,” *Conf. proc. IEEE Power Electronics Specialists,* pp. 2736-2741, 2004.

[10] L.Svilainis and V. Dumbrava, “Evaluation of the ultrasonic transducer electrical matching performance,” *ULTRAGARSAS,* vol.62, no.4, 2007.

[11] S. Butterworth, “On electrically-maintained vibrations,” *Proc.Phys. Soc. (London),* vol. 27, pp. 410–424, Dec. 1914–Aug. 1915.

[12] Z. Ru, E. Klumperink C. Saavedra and B. Nauta, “A tuable 300-800MHz RF sampling receiver achieving 60dB harmonic rejection and 0.8dB minimum NF in 65nm CMOS,” *Radio Frequency Integrated Circuits Symposium,* pp. 21-24, 2009.

[13] M. Dielacher, M. Flatscher, and W. Pribyl, “A low noise amplifier with on-chip matching network and integrated bulk acoustic wave resonators for high image rejection,” *Research in Microelectronics and Electronics,* 2009. PRIME 2009, pp. 172–175, Jul. 2009.

[14] N. Sun, Y. Liu, H. Lee, R. Weissleder, and D. Ham, “CMOS RF biosensor utilizing nuclear magnetic resonance,” *IEEE J. Solid-State Circuits,* vol. 44, no. 5, pp. 1629–1643, May 2009.

[15] I. Kim, H. Kim, F. Griggio, R. L. Tutwiler, T. N. Jackson, S. T. Mckinstry, and K. Choi, "CMOS Ultrasound Transceiver Chip for High-Resolution Ultrasound Imaging Systems," *IEEE Transactions on Biomedical Circuits and Systems*, vol. 3, no. 5, October 2009